7 APPENDIX A:

NS-line, Krafla-FIRE, 1994

deployment KRNS					
Nanometrix calibration				Rugby calibration time	
PRS/stat.	download	upload	drift		
0209/P15	207:11:04	212:09:27	+0.013	207:11:14:59.98	208:18:13:59.99
				210:09:44:59.99	212:09:20:59.99
0243/P14	207:10:42	212:13:45	−0.193	207:10:48:59.99	208:18:31:59.93
				210:10:05:59.87	212:13:24:59.78
0211/P13	207:10:11	212:13:44	−0.218	207:10:19:59.99	208:18:44:59.92
				210:10:15:59.87	212:13:26:59.75
0216/P12	207:10:30	208:20:46	+0.008	207:14:44:59.98	
0217/P11	207:10:24	209:11:01	−0.039	207:10:30:59.99	209:10:49:59.94
		212:13:47	−0.095	210:10:50:59.92	212:13:30:59.88
0013/P10	207:11:01	209:11:11	−0.121	207:11:11:59.98	209:10:50:59.86
0019/P9	207:10:48	209:11:14	−0.182	207:10:55:59.98	209:10:57:59.80
0017/P8	207:10:58	209:11:12	−0.014	207:11:07:59.98	209:10:54:59.97
0010/P7	207:10:52	209:12:07	+0.036	207:10:59	209:11:47
0016/P6	207:10:44	209:18:45	−0.083	207:10:52:59.99	209:18:18:59.91
0015/P5	207:10:20	209:18:35	−0.017	207:10:24:59.98	209:18:12:59.98
0018/P4	207:10:37	209:18:43	+0.001	207:10:44:59.98	208:16:51:59.98
				209:18:32:59.99	
0012/P3	207:10:00	209:18:39	+0.050	207:10:15:59.98	208:16:40:60.01
				209:18:23:60.04	
0014/P2	207:09:56	209:18:23	+0.024	207:10:10:59.98	208:16:14:60.00
				209:17:50:60.01	
0187/P1*	207:10:34	212:13:12	−0.134	207:10:40:59.98	208:15:04:59.95
				212:12:56:59.84	
0187/PD*	207:10:34	212:13:12	−0.134	207:10:40:59.98	208:15:04:59.95
				212:12:56:59.84	
0056/PA	207:18:14	dead			
0072/PB	207:11:32	209:18:33	−0.228	207:11:43:59.98	208:14:44:59.87
				209:17:56:59.77	
0048/SS	207:11:36	208:21:19	−0.047	207:11:39:59.98	209:20:19:59.93
		209:20:25	−0.072		
0036/PS	207:11:11	209:12:01	+0.042	207:11:17	209:11:52:60.02
0240/PG	207:10:55	209:12:13	−0.173	207:11:04:59.98	209:11:51:59.81

* 0187 was moved from P1 to PD jday 209, without a new deployment code

N-S.line, Krafla-FIRE, 1994

deployment KRN1						
Nanometrix calibration				Rugby calibration time		
PRS/stat.	download	upload	drift			
0216/P12	209:09:26	212:13:50	+0.036	209:09:29:59.98	210:10:29:59.99	212:13:29:60.01
0013/P10	209:11:33	212:16:00	−0.188	209:11:49:59.99	210:11:05:59.92	
0019/P9	209:11:38	212:15:34	−0.276	209:11:41:59.98	210:11:13:59.89	
0017/P8	209:11:35	212:11:02	−0.017	209:11:44:59.98	210:11:22:59.98	
0010/P7	209:13:02	212:10:26	+0.051	209:13:17:59.98	210:11:32:60.00	
0016/P6	209:19:51	212:12:03	−0.097		210:14:12:59.96	212:12:01:59.65
0015/P5	209:19:49	212:12:15	−0.014		210:14:28:59.98	212:12:02:59.96
0240/P4	209:13:07	212:12:30	−0.252	209:13:14:	210:14:38:	212:12:11:
0014/P3	209:19:46	212:11:49	+0.036		210:14:48:60.00	
0012/P2	209:19:54	212:14:21	+0.079		210:15:04:60.01	
0048/PA	209:20:43	212:14:23	−0.078		210:15:16:59.96	
0036/PC	209:13:05	212:12:53	+0.045	209:13:18:59.98		
0056/PS	209:22:13	212:15:05	+0.022	209:22:16:59.98	210:13:45:59.98	
0072/PG	209:20:12	212:15:06	−0.256		210:13:59:59.92	212:15:10:59.71
0018/SS	209:19:58	210:08:31	+0.002		210:12:05:59.98	211:19:19:59.99
		212:09:06	+0.005			

E-W.line, Krafla-FIRE, 1994

deployment KREV					
Nanometrix calibration				Rugby calibration time	
PRS/stat.	download	upload	drift		
0072/porch	214:14:58	215:14:49	−0.112	214:15:04:60.00	
0209HRH	214:09:57	216:09:52	−0.001		216:09:20:60.00
0048/GIL	214:14:53	216:09:54	−0.061	214:15:02:60.00	216:09:17:59.94
0056/PG	214:17:08	216:09:57	−0.011		216:09:18:59.99
0014/H-10	214:15:09	216:09:11	+0.016	214:17:06:60.00	216:08:56:60.02
0015/V2	214:15:00	216:09:10	−0.016	214:17:04:60.00	216:08:53:59.98
0012/V3	214:14:51	216:11:04	+0.046	214:15:01:60.00	216:10:59:60:05
0016/L1	214:15:46	216:11:13	−0.061	214:17:03:60.00	216:11:11:59.94
0019/L2	214:09:54	216:11:45	−0.178		216:11:43:59.82
0211/L3	214:09:42	216:11:43	−0.086	214:09:47:59.99	216:11:41:59.91
0187/L4	214:10:34	216:12:43	−0.056		216:12:30:59.94
0243/L5	214:10:39	216:12:41	−0.089		216:12:37:59.91
0217/HVA	214:09:46	217:17:01	−0.085	214:09:49:59.99	217:16:57:59.91
0216/MUL	214:09:39	217:17:05	+0.023	214:09:43:59.99	217:17:01:60.02
0240/TJA	214:09:44	217:17:03	−0.291	214:09:48:59.99	217:17:00:59.70
0010/BOG	214:10:55	217:16:41	+0.011		216:16:38:60.01
0013/BOH	214:10:44	217:16:43	−0.143		216:16:39:59.85
0017/BON	214:10:57	217:16:48	−0.034		216:16:44:59.96
0036/ÁRE	214:10:51	217:16:54	+0.007	214:14:47:59.96	216:16:51:60.00
0018/SS				214:14:41:60.00	216:09:29:60.00
KRW50010/SS	217:15:43	218:10:57	+0.006	217:15:46:59.99	218:08:45:60.00
KRW50072/SS	218:13:40	218:22:31	−0.055	218:13:42:59.98	

deployment KRW2

Nanometrix calibration				Rugby calibration time	
PRS/stat.	download	upload	drift		
0211/HRH	216:11:53	219:12:46	−0.125	216:12:00:60.00	219:12:31:59.88
0016/GIL	216:11:31	219:12:52	−0.108	216:11:35:60.00	219:12:49:59.89
0012/PG	216:11:22	219:12:41	+0.064	216:11:31:59.99	219:12:34:60.06
0013/H-10	216:16:53	217:11:47	−0.050		217:11:45:59.95
0010/V2	216:16:46	217:15:28	+0.008		217:15:24:60.01
0056/V3	216:10:14	219:17:09	−0.014	216:10:21:60.00	219:16:30:59.99
0048/L1	216:10:04	219:13:38	−0.106	216:10:06:60.00	219:13:31:59.89
0015/L2	216:09:51	219:13:37	−0.037	216:09:59:60.00	219:13:29:59.96
0018/L3	216:10:10	219:12:48	−0.000		219:12:41:60.00
0014/L4	216:09:49	219:12:47	−0.001	216:09:52:59.99	219:13:39:60.02
0209/L5	216:10:01	219:12:50	+0.009	216:10:03:60.00	219:12.46:60.00
0019/BOG	216:11:56	219:20:51	−0.270	216:12:00:59.99	219:20:21:59.73
0187/BOH	216:12:53	219:20:50	−0.074	216:12:57:59.99	219:20:20:59.93
0243/BON	216:12:50	219:20:48	−0.146	216:12:54:59.99	219:20:16:59.85

E-W.line, Krafla-FIRE, 1994

deployments KRW4 and KRW5

Nanometrix calibration				Rugby calibration time	
PRS/stat.	download	upload	drift		
0017/HVA	217:11:27	219:20:54	−0.028	217:11:46:59.99	219:20:22:59.97
0036/MUL	217:11:43	219:20:56	−0.000		219:20:23:59.99
0013/TJA	217:12:05	219:20:58	−0.135	217:12:12:60.00	219:20:26:59.86
0240/H10	217:17:15	219:09:40	−0.158	217:17:17:59.99	219:09:33:59.84
0217/V2	217:17:11	219:09:42	−0.046	217:17:13:59.99	219:09:39:59.95
0216/H18	217:17:31	219:12:54	+0.009		219:12:36:60.01
0010/GEI	218:13:37	219:20:53	−0.00		219:20:18:60.00
KRW50010/SS	217:15:43	218:10:57	+0.006		
KRW50072/GEI	215:15:46	no drift available for deployment krw50072			
KRW50072/SS	218:13:40	218:22:31	−0.055		

E-W.line, Krafla-FIRE, 1994

NANOMETRIX CLOCKS; CALIBRATION WITH RUGBY SIGNAL

CLOCK 033, SHOTSITE CLOCK

DATE	DRIFT	TIME OF CALIBRATION	CORR (sec)
27/7	207:08:30		
27/7	0.017 AHEAD	208:09:30	−0.017
27/7	0.000 AHEAD	208:11:55	−0.000
28/7	0.009 AHEAD	209:08:30	−0.009
29/7	0.009 AHEAD	210:12:00	−0.009
04/8	0.018 AHEAD	216:09:30	−0.018
05/8	0.017 AHEAD	217:10:00	−0.017
06/8	0.009 AHEAD	218:08:00	−0.009
06/8	4.000 LATE	218:13:30	+4.000
06/8	4.000 LATE	218:22:00	+4.000

CLOCK 009

DATE	DRIFT	TIME OF CALIBRATION	CORR (sec)
27/7	207:08:30		
27/7	0.049 LATE	208:09:30	+0.049
27/7	0.049 LATE	208:11:55	+0.000
27/7	0.024 LATE	208:20:40	+0.024
28/7	0.016 LATE	209:08:30	+0.016
28/7	0.016 LATE	209:18:00	+0.016
29/7	0.032 LATE	210:12:00	+0.032
30/7	0.049 LATE	211:12:30	+0.049
30/7	0.000 LATE	211:19:00	+0.000
31/7	0.032 LATE	212:09:00	+0.032
31/7	0.025 LATE	212:17:30	+0.025
01/8	0.066 LATE	213:22:21	+0.066
02/8	0.016 LATE	214:09:00	+0.016
02/8	0.016 LATE	214:14:20	+0.016
04/8	0.041 LATE	216:09:00	+0.041
04/8	0.016 LATE	216:17:00	+0.016
05/8	0.032 LATE	217:10:00	+0.032
05/8	0.008 LATE	217:15:30	+0.008
06/8	0.032 LATE	218:09:00	+0.032

Figure 1. Volcanic systems in the Neovolcanic zones of Iceland. Each system consists of a central volcano (shaded region) and a transecting fault swarm (dotted region). Some central volcanoes have developed calderas (circular arcs). Inset shows Krafla central volcano. Note stations (filled circles) and events (numbered open trianges) used in this study: 1. Langjökull earthquake; 2. Eyjafjördur shotsite; 3. Skjálfandi shotsite; 4. 1991 Axarfjördur shotsite; 5. 1994 Axarfjördur shot; 6. Axarfjördur earthquake; 7. Sænautavatn shotsite; 8. Askja shotsitde; 9. Lögurinn shotsite; 10. Reydarfjördur shotsite; 11. Gæsadalur shotsite; 12. Leirhnúkur shotsite; and 13. Víti shotsite. Basemap after Einarsson and Sæmundsson [1987].

Figure 2. S waves observed in RRISP data (after Gebrande et al., 1980). Record sections, reduced to 3.98 km/s, from shotpoint E (top) in NE-Iceland recorded at RRISP profile I, also in northeastern Iceland, and from shotpoint G (bottom) in south Iceland recorded along RRISP profile II in southeastern Iceland. The record sections are made up of horizontal and some vertical components. S wave arrival time, estimated from $V_p/V_s = 1.76$, is plotted as a dashed line. Gebrande et al. [1980] state that the S wave is delayed or attenuated at ranges greater than 140-170 km. Note, however, an interval of 2 S wave arrivals in the top profile.

Figure 3. P waves observed in RRISP data, after Gebrande et al. [1980]. A vertical-component record section, reduced to 7 km/s, from shotpoint G in south Iceland, recorded at RRISP profile II in southeastern Iceland. Note the 0.5s offset between seismograms from the two component shots, G1 and G2, which are interleaved on the record section. P-wave readings from the regional Iceland seismic network (G1, filled circles; G2, shaded circles) arrive earlier by about 0.5s.

Figure 4. Tectonic map of the Krafla central volcano showing the caldera rim (bold curve), fissures and faults (lines), 1724-1729 lava flows (shaded areas), seismic stations (small circles), and shotpoints (large circles).

Figure 5. Geological cross sections of the Leirbotnar-Hvíthólar (A) and Leirbotnar-Sudurhlídar (B) geothermal fields, as derived from drillhole cuttings. After Ármannsson et al. [1987].

Figure 6. Compressional wave traveltimes versus range. A) P wave traveltimes for the 1993 EW profile, within the Krafla central volcano from the Gæsadalur (filled dots) and Víti (crosses) shotsites. The similarity of traveltimes is evidence against strong lateral heterogeneity. B) P wave traveltimes for the NW profile within the Krafla central volcano, from shots in Víti recorded to the north (crosses) and south (dots). Calculated traveltime for the one-dimensional KRA-73 (thin line) and KRA-93 (thick line) crustal models are shown.

Figure 7. One-dimensional models of the compressional velocity within the Krafla central volcano. A high resolution model (bold curve), derived from the 1993 EW profile, has two low velocity zones. The older, KRA73 model (fine curve) is shown for comparison.

Figure 8. Vertical-component record section, reduced to 5 km/s, from the Víti shotsite recorded on the 1993 EW profile within the Krafla central volcano. Note two breaks in the P wave arrival times (solid lines) at 3 and 5 km range, interpreted as being due to low velocity zones.

Figure 9. Two-dimensional, NS compressional velocity model across the eastern part of the Krafla caldera derived from data from the Víti shotsite (V). The model is 25 km long and 5 km deep. The data constrain the uppermost 2 km. Colorbar denotes variations in compressional velocity.

Figure 10. Two-dimensional, EW compressional velocity model across the central part of the Krafla caldera derived from the Gæsadalur (G), Leirhnúkur (L), and Víti (V) shotsites. The model is 15 km long and 3 km deep. The data constrain the uppermost 2 km, between the shotsites. Colorscale denotes variations in compressional velocity.

Figure 11. P wave traveltimes for the NS (Figure 9) and EW (Figure 10) profiles within the Krafla central volcano. Data (squares), predictions of our model (solid lines) and from Arnott and Foulger's [1994] model (dotted lines) are shown. Note that Arnott and Foulger's [1994] calculated traveltimes are generally early by 0.1-0.4s. A) NS profile from the Víti shotsite. B) EW profile from the Gæsadalur (at 5 km), Leirhnúkur (12 km), and Víti (14 km) shotsites. C) Enlargement of the central part of EW profile.

Figure 12. Radial horizontal-component record section, reduced to 5 km/s, from the Gæsadalur shotsite recorded on the 1993 EW profile. Lines show observed P wave arrivals and calculated S-wave arrival (estimated from V_p/V_s ratio = 1.76). Note that the actual S wave arrival fits the prediction well, even out to ranges beyond the two P-wave shadow zones (3.7 and 5.6 km), indicating that no layers of melt have been encountered by the S wave.

Figure 13. A hypothetical crustal model showing a laterally homogeneous crust (0-10 km) and a laterally heterogeneous crust (10-20 km). The star at 10 km denotes an earthquake at 1.5 km depth. Colorbar shows variations in compressional velocity.

Figure 14. Calculated traveltime curves for a 3 km deep (bold line) and 1.5 km deep (thin line) earthquake at 10 km range in the model in Figure 13. Raypaths at 0-10 km have travelled through a laterally homogeneous crust whereas raypaths at 10-20 km have travelled through a laterally heterogeneous crust.

Figure 15. Vertical-component record section, reduced to 6.5 km/s and band-passed 2-8 Hz, from the Axarfjördur (A) and Askja (B) shotsites on the northern and southern ends, respectively, of the 1994 NS profile. The two sections have been alligned with respect to the caldera. Note the clear P wave on the flank of the caldera nearest the shotsite, and the region of low amplitudes within the caldera.

Figure 16. Vertical-component record section, reduced to 6.5 km/s and band-passed 2-8 Hz, from the Eyjafjördur (A) and Lögurinn (B) shotsites on the western and eastern ends, respectively, of the 1994 EW profile. Note the clear P wave on the flank of the caldera nearest the shotsite, and the region of low amplitudes within the caldera.

Figure 17. Summary of P wave first arrival picks from events on the 1994 NS profile: LANG, Langjökull earthquake; ASKJA, Askja shotsite; AXEQ, Axarfjördur earthquake; AX, 1994 Axarfjördur shotsite. The profile crosses the Víti crater at a distance of zero. Numbers accompanying event name refer to the distance of the event. The traveltime curves have a broad (10-15 km) high-velocity(-0.2s) anomaly centered over the Krafla central volcano, on which localized (1-3 km) slow (0.1-0.3s) anomaly is superimposed. The low-velocity anomaly is evident on only some of the profiles (e.g. LANG).

Figure 18. Summary of P wave first arrival picks from events on the 1994 EW profile: REYD, Reydarfjördur shotsite; LOGU, Lögurinn shotsite; SAEN, Sænautavatn shotsite; SKJA, Skjálfandi shotsite; and EYJA, Eyjafjördur shotsite. The profile crosses the Víti crater at a distance of zero. Numbers accompanying event name refer to the distance of the event. The traveltime curves have a broad (10-15 km) fast (-0.2s) anomaly centered over the Krafla central volcano, on which localized (1-3 km) slow (0.1-0.3s) anomaly is superimposed.

Figure 19. Vertical-component record section, reduced to 7.0 km/s and low-passed beneath 7 Hz, from the Langjökull earthquake. Note the 0.3s delay of the P wave in a 3 km wide region at the center of the caldera, at ranges 223-226 km.

Figure 20. Vertical-component record section, reduced to 6.5 km/s and low-passed beneath 10 Hz, from a shot in Skjálfandi bay in north Iceland, recorded on the EW profile. The station density in highest within the Krafla caldera, at a range of 50-56 km. Apparent P velocity increases steadily towards the caldera where is becomes more irregular. A clear P_{ref} phase (deep crustal reflection) is observed on stations on the eastern flank of the central volcano.

Figure 21. Vertical-component record section, reduced to 6.5 km/s and band-passed 2-8 Hz, of A) a shot in Axarfjördur observed on the 1994 NS profile which crosses the eastern part of the Krafla caldera, and B) a shot in Axarfjördur observed on the 1991 NS profile along the western part of Krafla caldera. Note the significant difference in character of the two record sections. The apparent P velocity is markedly higher along the 1994 profile at 60-65 km range, whereas the deep crustal reflection, P_{ref}, is clearest on the 1991 profile.

Figure 22. Radial-component record section, reduced to 4.0 km/s and lowpassed beneath 10 Hz, of a shot in Skjálfandi recorded on the EW profile. Observed arrival times of P and P_mP are shown, as are predicted arrival times for S and S_{ref} based on V_p/V_s=1.76. Note that close agreement between predicted and observed S arrival times, at least out to a range of 50 km. Beyond these ranges the S wave is attenuated by caldera structures.

Figure 23. Radial-component record section, reduced to 4.5 km/s, of A) a shot in Eyjafjördur and B) a shot in Lögurinn, both observed on the EW profile. Note that the amplitude of the S wave is sharply reduced at ranges greater than 73 km in A and 113 in B, suggesting a zone of high attenuation within the caldera.

Figure 24. Transverse-component 'fan' sections of A) Axarfjördur earthquake observed on the EW profile; and B) Eyjafjördur shot observed on the NS profile. The caldera rims and the Víti shotsite are shown for reference. The A fan misses the the northern edge of the S wave shadow by about 1 km. The B profile crosses a S wave shadow, at 5.1 km, which is less than 2 km wide and centered near the Víti crater.

Figure 25. Radial-component record section, reduced to 4.37 km/s, of the Langjökull earthquake observed on the NS profile. A) Lowpassed (0.5 Hz) record-section reveals a pulse in the S wave that can be correlated across the array. This phase arrives 0.2s early, with repect to the 4.26 km/s reference line, in the 220-226 distance range, which corresponds to the caldera rim, and 0.5s late in the 226-228 distance range, which corresponds to the central part of the caldera. Compare also with P delays in figure 19. B) Unfiltered record section for comparison.

Figure 26. Radial-component record section, reduced to 4.0 km/s, of the Eyjafjördur detonation (73.2 km from Víti) observed on the EW profile, showing S wave (shadowed at ranges greater than 76 km) and S_{ref} deep crustal reflection. A) Bandpassed (0.5-2.0 Hz); B) Unfiltered.

Figure 27. Radial-component record section, reduced to 4.5 km/s, of the Axarfjördur earthquake (60.2 km from Víti) observed on the NS profile, showing S wave (shadowed at ranges greater than 62 km) and S_{ref} deep crustal reflection. A) Unfiltered; B) Bandpassed (0.5-2.0 Hz).

Figure 28. Crustal structure of the Krafla Central Volcano. Two-dimensional, NS compressional velocity model derived from traveltime data from the Axarfjördur (X) and Askja (A) shotsites, and the Axarfjördur earthquake (X). The Víti shotsite is marked with a V. The model is 200 km long and 25 km deep. Our receivers are located in the 56-78 km range. P wave and P_{ref} wave raypaths from individual shotsites show which part of the model is constrained by the data. Colorbar denotes variations in compressional velocity. Only the part of the model beneath the central volcano itself is well-resolved.

Figure 29. Crustal structure across the Krafla Central Volcano. Two-dimensional, EW compressional velocity model derived from traveltime data from the Eyjafjördur (E), Sænautavatn (S), Lögurinn (L), and Reydarfjördur (R) shotsites. The Víti shotsite is marked with a V. The model is 225 km long and 30 km deep. Our receivers are located in the 48.6-104.3 km range. P wave and P_{ref} wave raypaths from individual shotsites show which part of the model is constrained by the data. Colorbar denotes variations in compressional velocity. Only the part of the model beneath the central volcano itself is well-resolved.

Figure 30. P wave traveltime data from the NS (Figure 28) profile, along the NVZ. The profile crosses the Víti crater at a distance of zero. Numbers accompanying event name refer to the distance of the event. Data (triangles) and the calculated P wave and P_{ref} arrivals (dotted lines). Shown from the top are; the Axarfjördur (AX) shot, the Axarfjördur earthquake (AXEQ), and the Askja shot.

Figure 31. P wave traveltimes for the EW (Figure 29) profile, across the NVZ. The profile crosses the Víti crater at a distance of zero. Numbers accompanying event name refer to the distance of the event. Data (triangels) and the calculated P wave and P_{ref} arrivals (dotted lines). Shown from the top are; the Reydarfjördur (REYD), Lögurinn (LOGU), Sænautavatn (SAEN), and Eyjafjördur (EYJA) detonations.

Figure 32. Vertical-component record section, reduced to 6.5 km/s and band-passed 2-8 Hz, from the Axarfjördur earthquake. Note the 0.3-0.4s delay of the P wave southern part of the Krafla caldera, at ranges 61.5-71.0 km. A clear P_{ref} phase (deep crustal reflection) is observed on stations on the eastern flank of the central volcano. Compare to Figure 20.

Figure 33. Pálmason's [1963] crustal model of the Northern Volcanic Zone. The model is 350 km long, 5.5 km deep, and shows Pálmason's layers P-0 (2.8 km/s), P-1 (4.2 km/s), P-2 (5.1 km/s), and P-3 (6.3 km/s). Note the 200 km wide depression in layer P-3 in N-Iceland and the 70 km wide and 1 km high doming of layer P-3, which is centered on the Mývatn region.

Figure 34. S wave attenuation zones within the Krafla caldera, delineated by P/S energy ratios, in the 2-8 Hz band. Top) P/S energy ratios from the west (EYJA) and the east (LOGU). Bottom) P/S energy ratios from the north (AXEQ) and soutwest (LANG). Note the two, opposed axes in each plot, used to separate the curves. The profiles cross near the Vít crater, at a distance of 0. The S wave shadow zone extends from ranges -4 to +6, on the EW profile, with + being east, and from 4 to -3 on the NS profile. A parallax effect is evident on the NS profile.

Figure 35. The Krafla central volcano showing the S wave attenuation zones delineated by Einarsson [1978] (red shaded regions), along with earthquake epicenters during the inflation period of March-April 1977 (black circles), the January 1977 deflation event (blue circles), and the September 1977 deflation event (red circles). Light green bands indicate the width of P wave attenuation zones determined by this study. The P wave attenuation zones extend 3 km NS and 10 km EW. Basemap after Einarsson [1991].

Figure 36. Interpretive drawings of the Krafla central volcano. (left) Physical structure, (middle) Shear wave attenuation, and (right) dynamics.

Figure 37 Radial-component record sections, reduced to 3.75 km/s and band-passed 1-10 Hz, for two shotsites along the SIST profile, which crosses the Western Volcanic Zone (WVZ) in southwest Iceland. A) AK shotsite, west of the WVZ. B) JL shotsite, east of the WVZ. S wave traveltimes, predicted from V_p/V_s=1.79 (solid line) fits observed S arrival well. Strong shear wave arrivals are observed within the WVZ. Data courtesy IRIS Data Management Center.

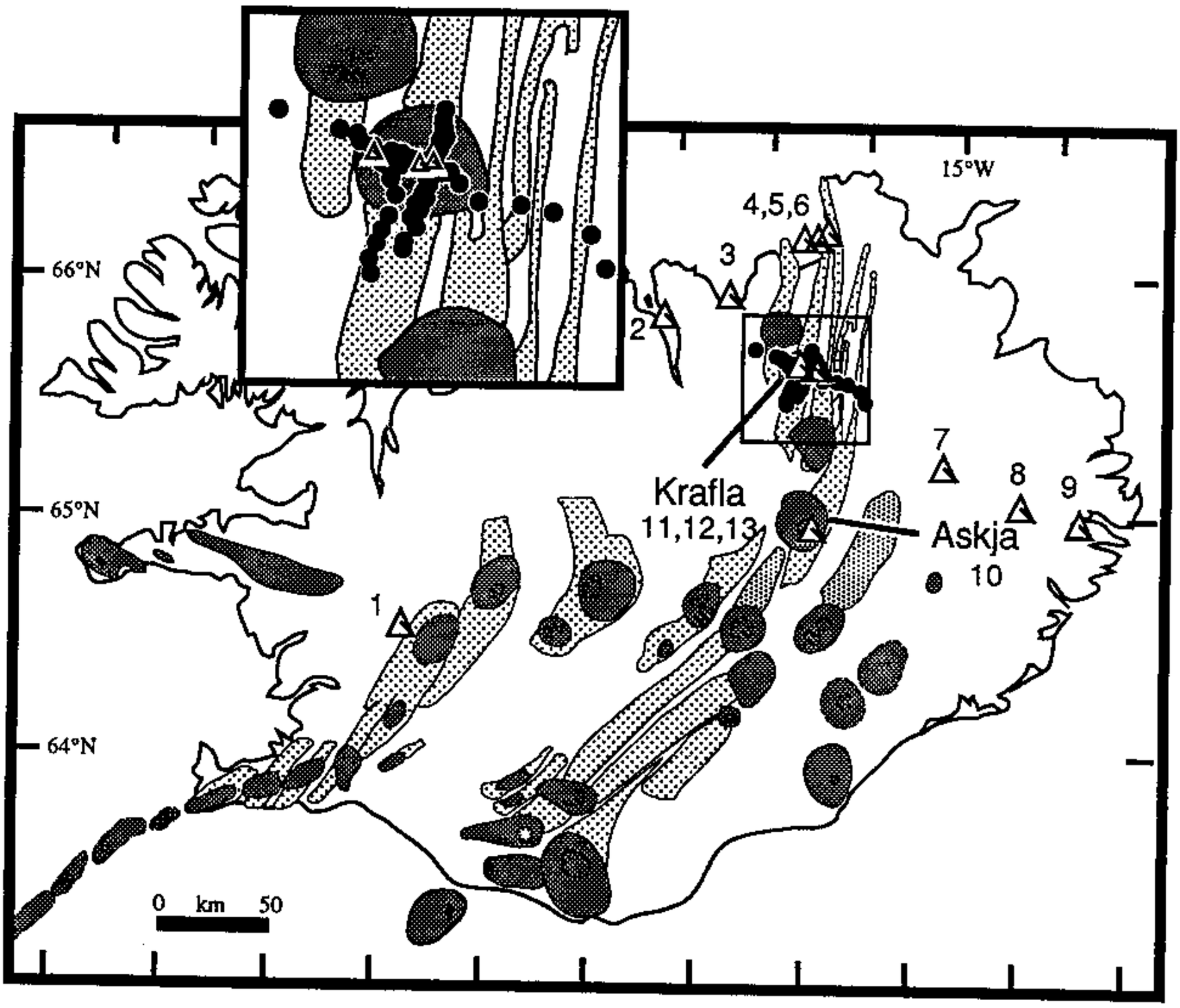

Figure 1

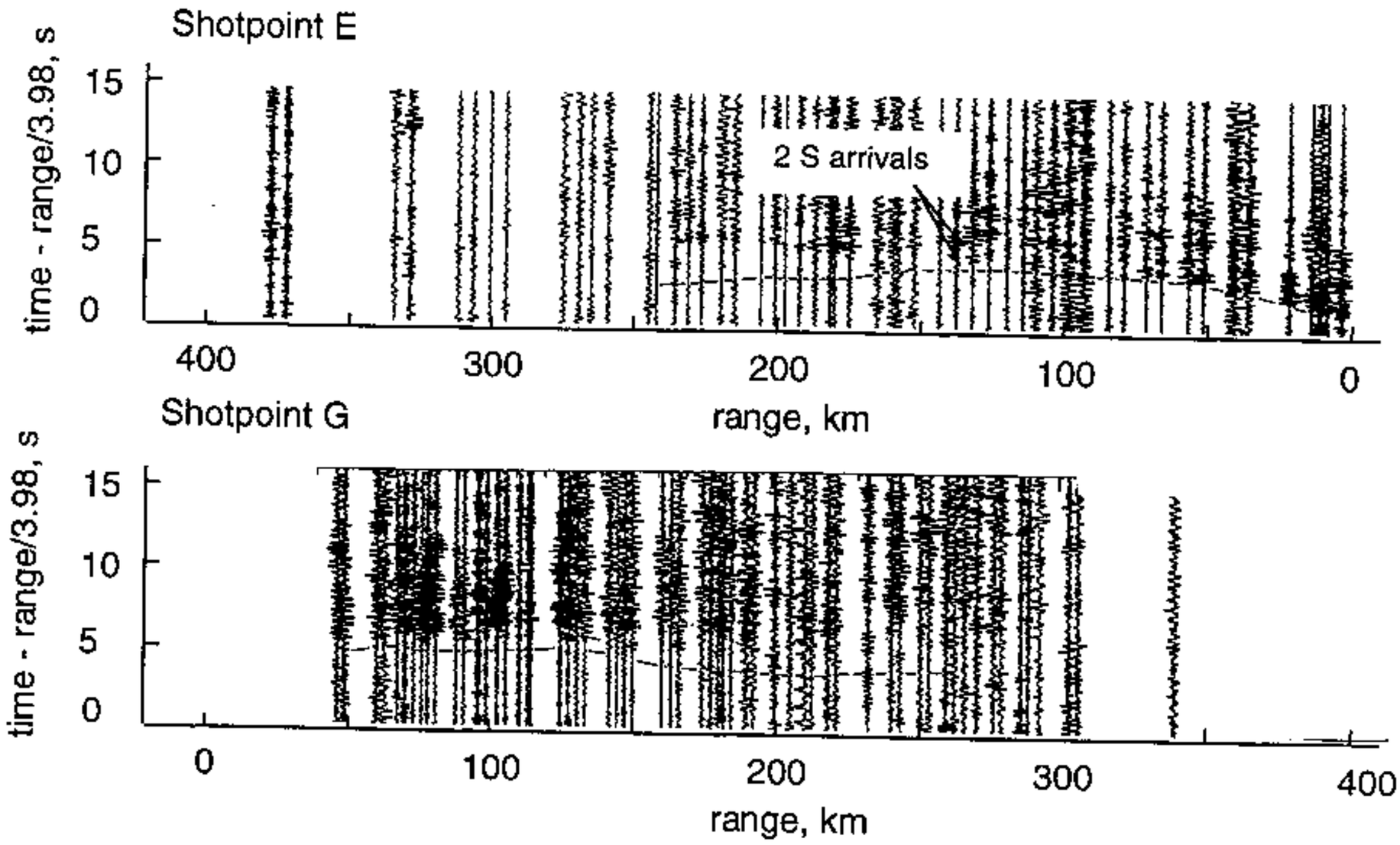
Shotpoint E
time - range/3.98, s
15
10
5
0
2 S arrivals
400
300
200
100
0
Shotpoint G
range, km
time - range/3.98, s
15
10
5
0
0
100
200
300
400
range, km

Figure 2

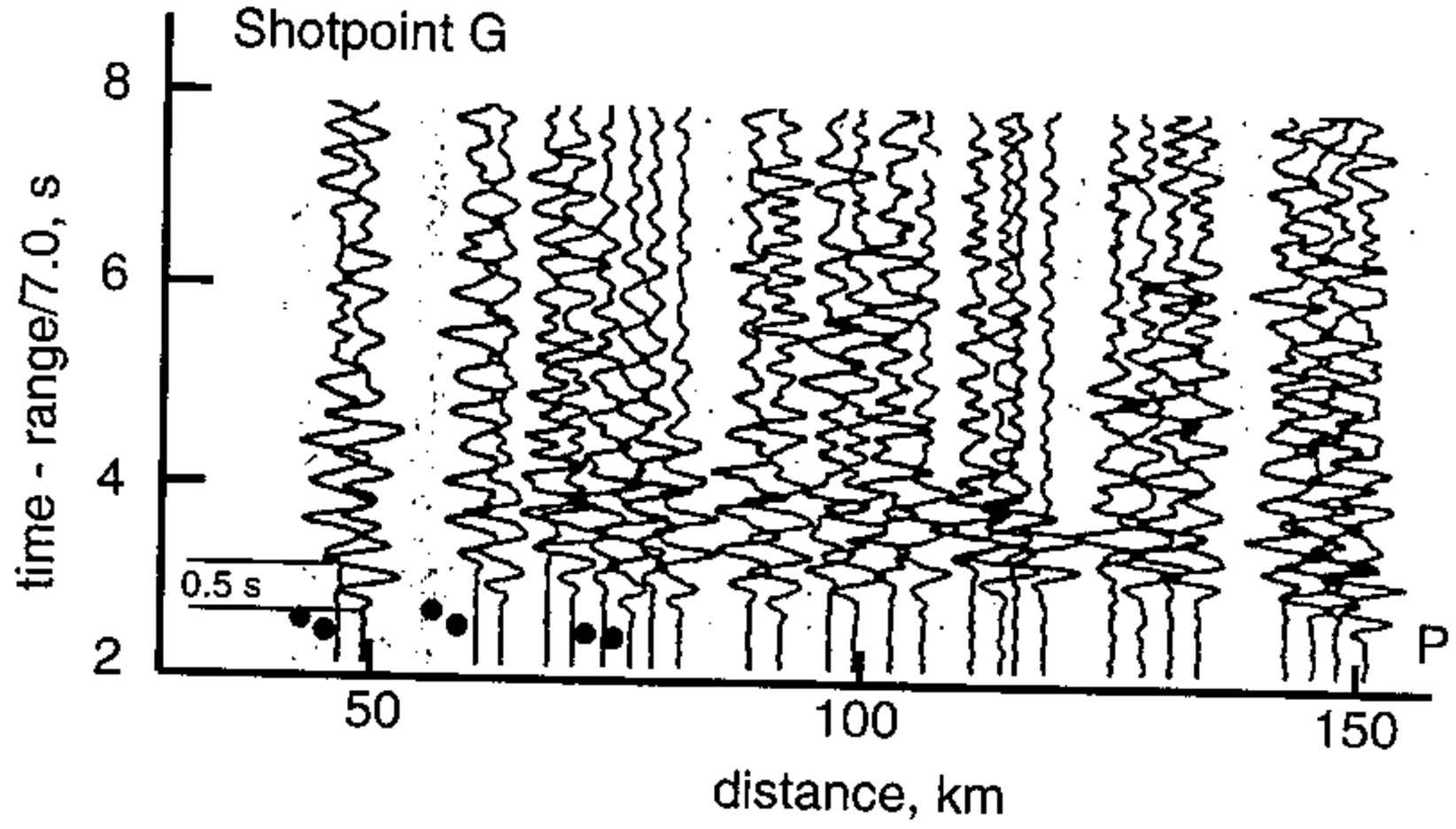

Figure 3

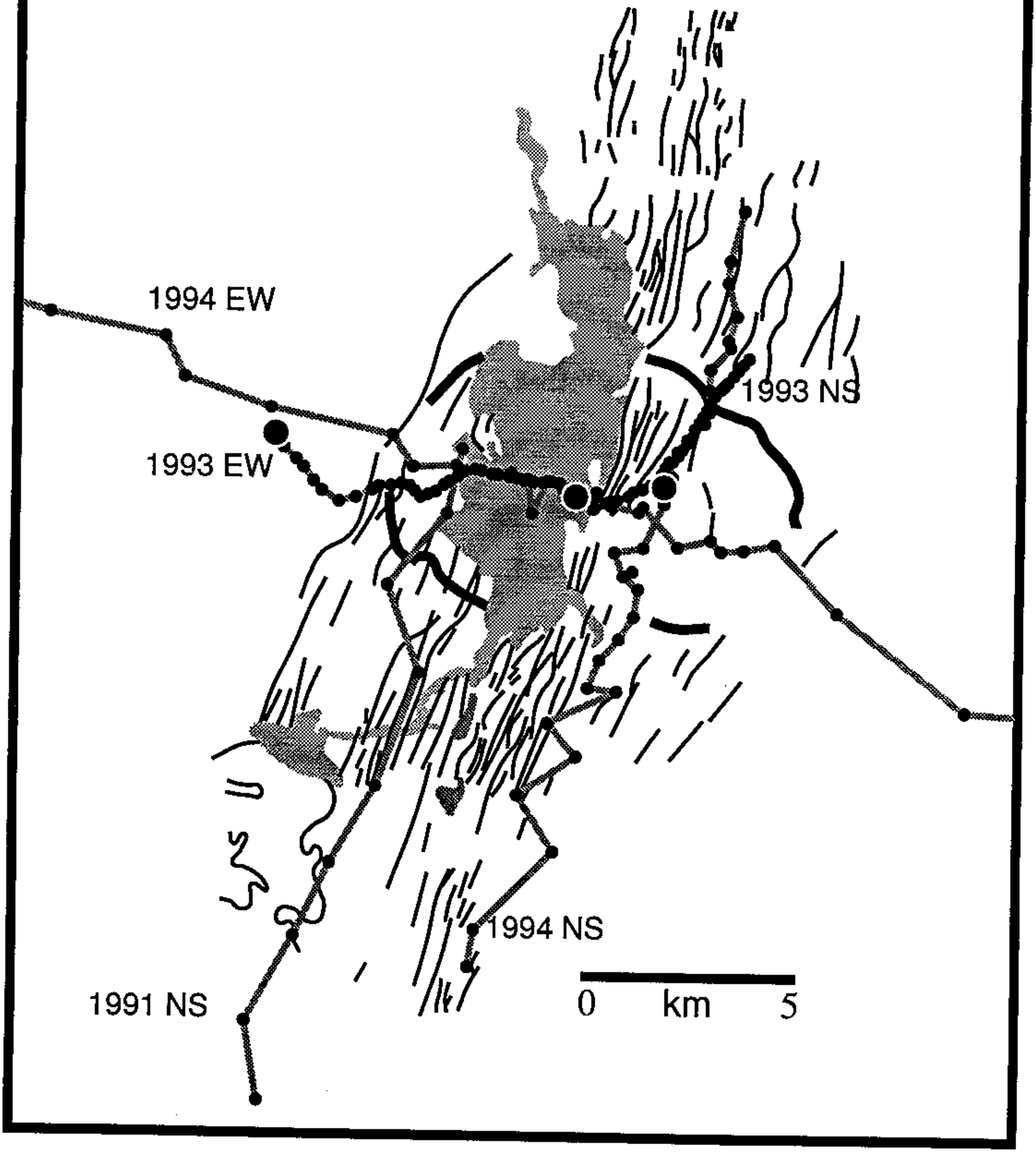

Figure 4

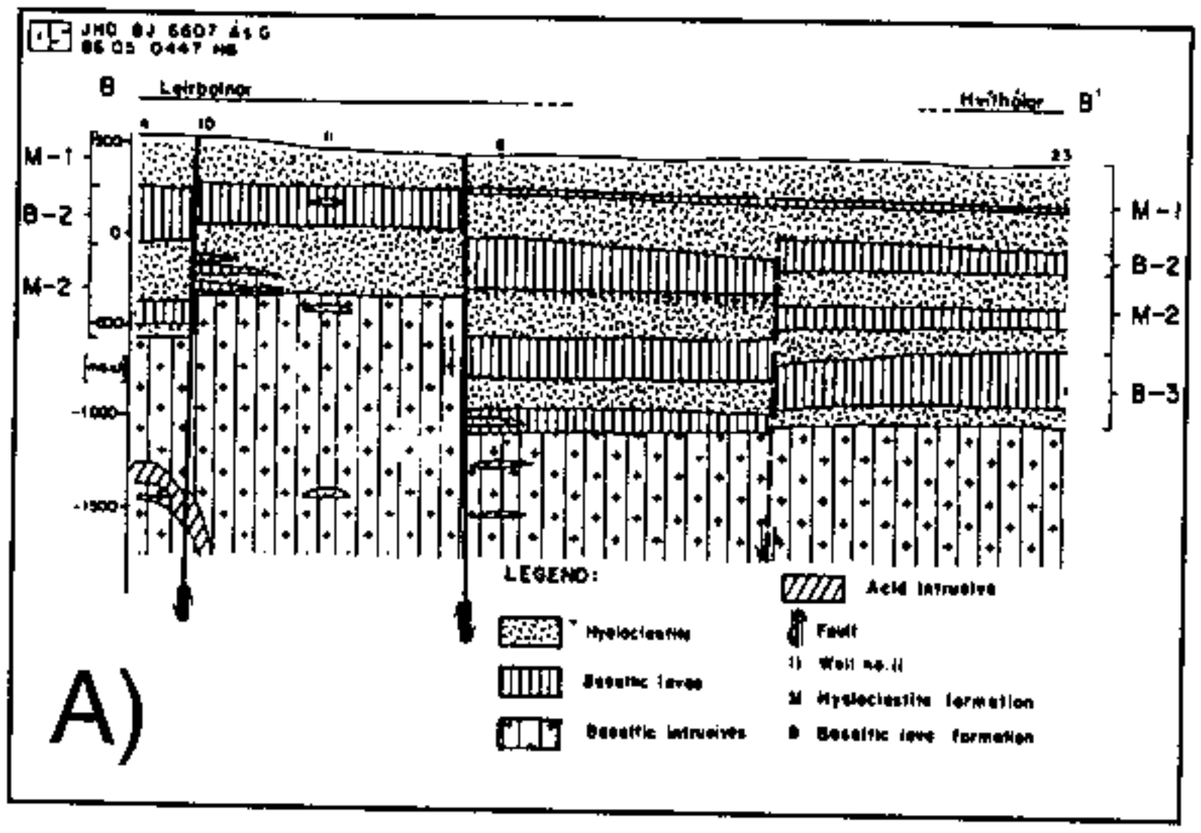
JHD BJ 6607 ÁsG
86 05 0447 HB
B
Leirbotnar
Hverahlíðar
B'
M-1
B-2
M-2
B-3
LEGEND:
Hyaloclastite
Basaltic lavas
Basaltic intrusives
Acid intrusives
Fault
1) Well no.1)
M Hyaloclastite formation
B Basaltic lava formation
A)

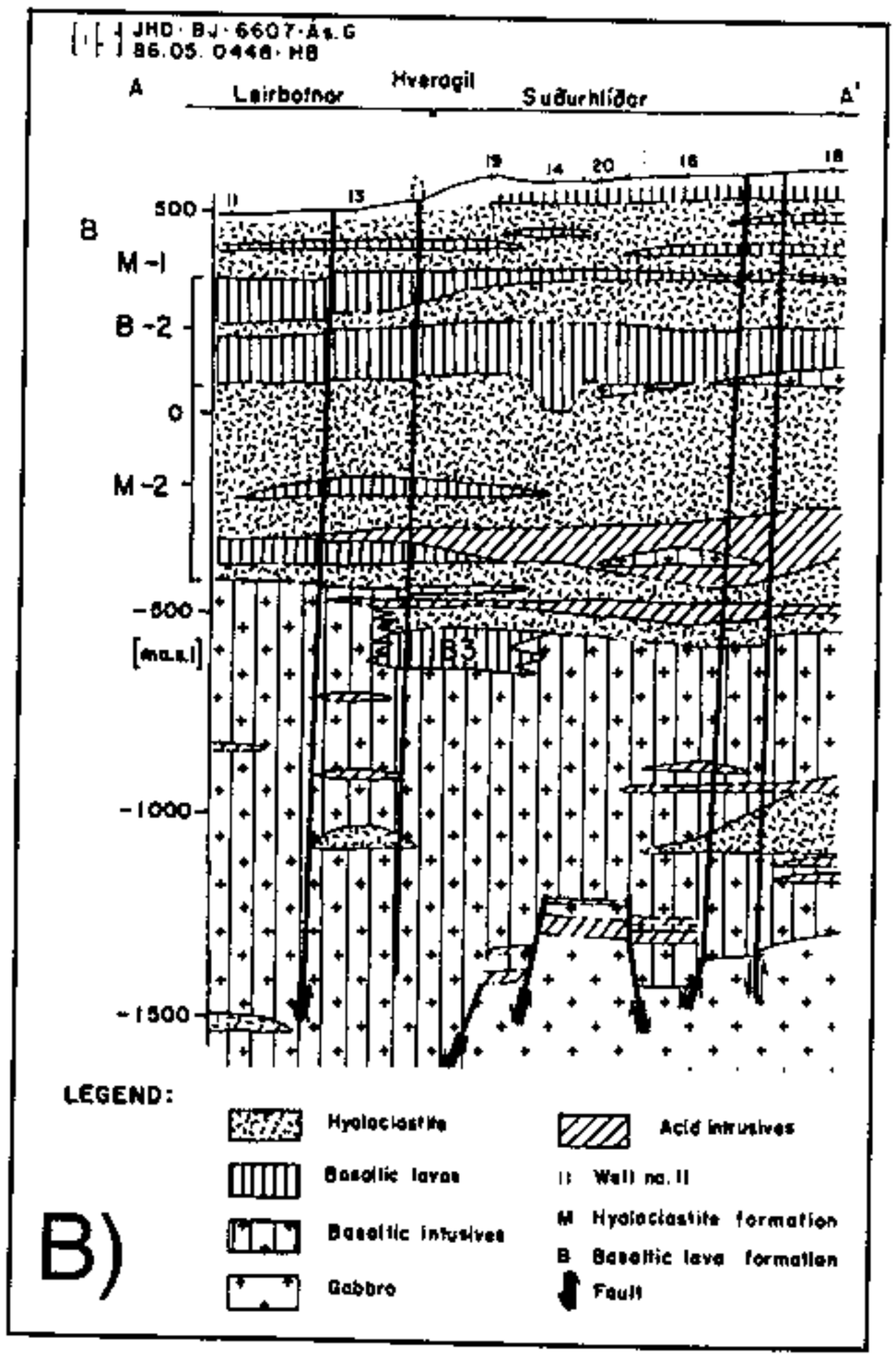
JHD · BJ · 6607 · Ás.G
86.05. 0448 · HB
A
Leirbotnar
Hveragil
Suðurhlíðar
A'
B
M-1
B-2
0
M-2
-500
[m.a.s.l]
B3
-1000
-1500
LEGEND:
Hyaloclastite
Basaltic lavas
Basaltic intrusives
Gabbro
Acid intrusives
I: Well no. II
M Hyaloclastite formation
B Basaltic lava formation
Fault
B)

Figure 5

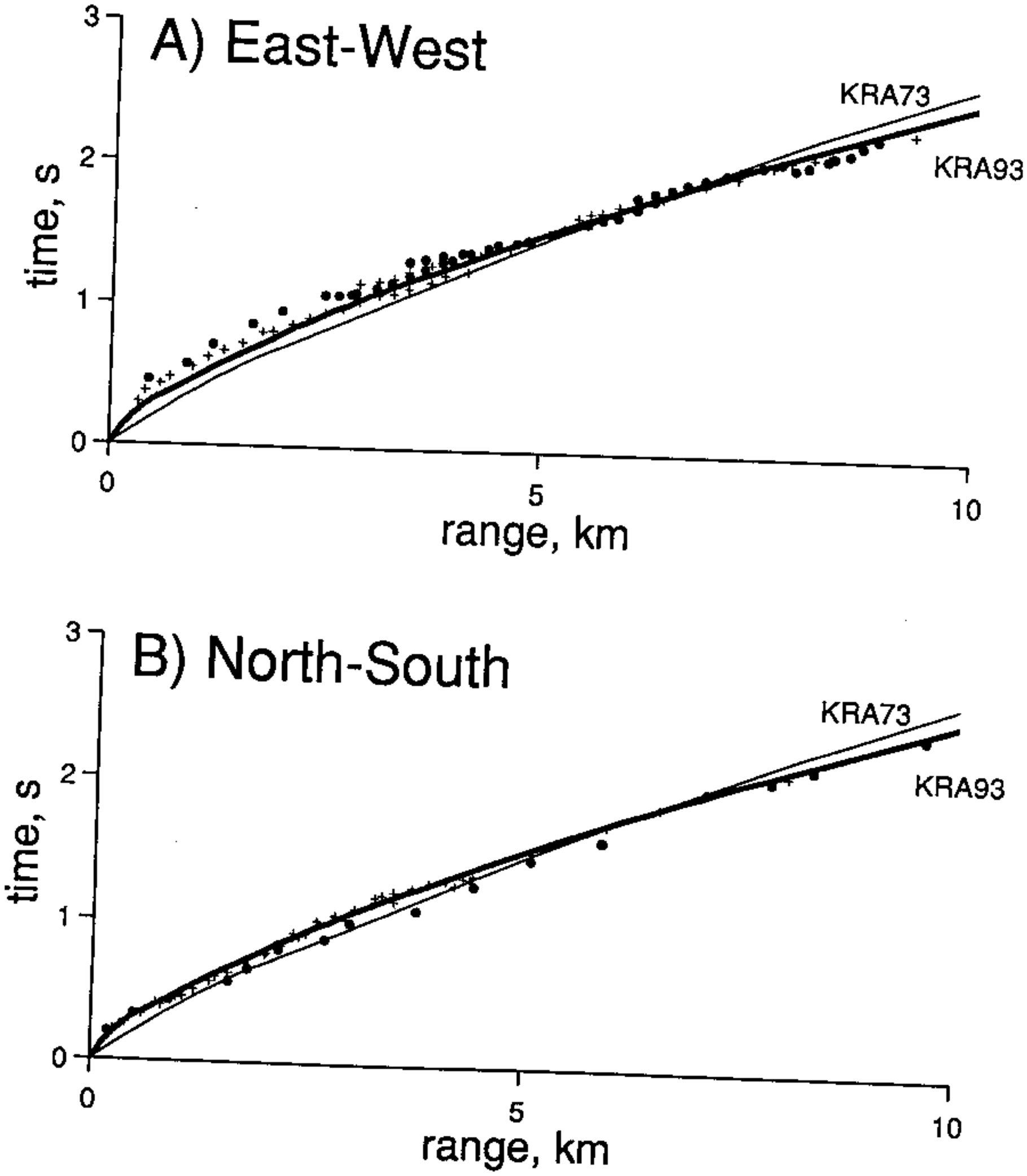
A) East-West
KRA73
KRA93
time, s
range, km
B) North-South
KRA73
KRA93
time, s
range, km

Figure 6

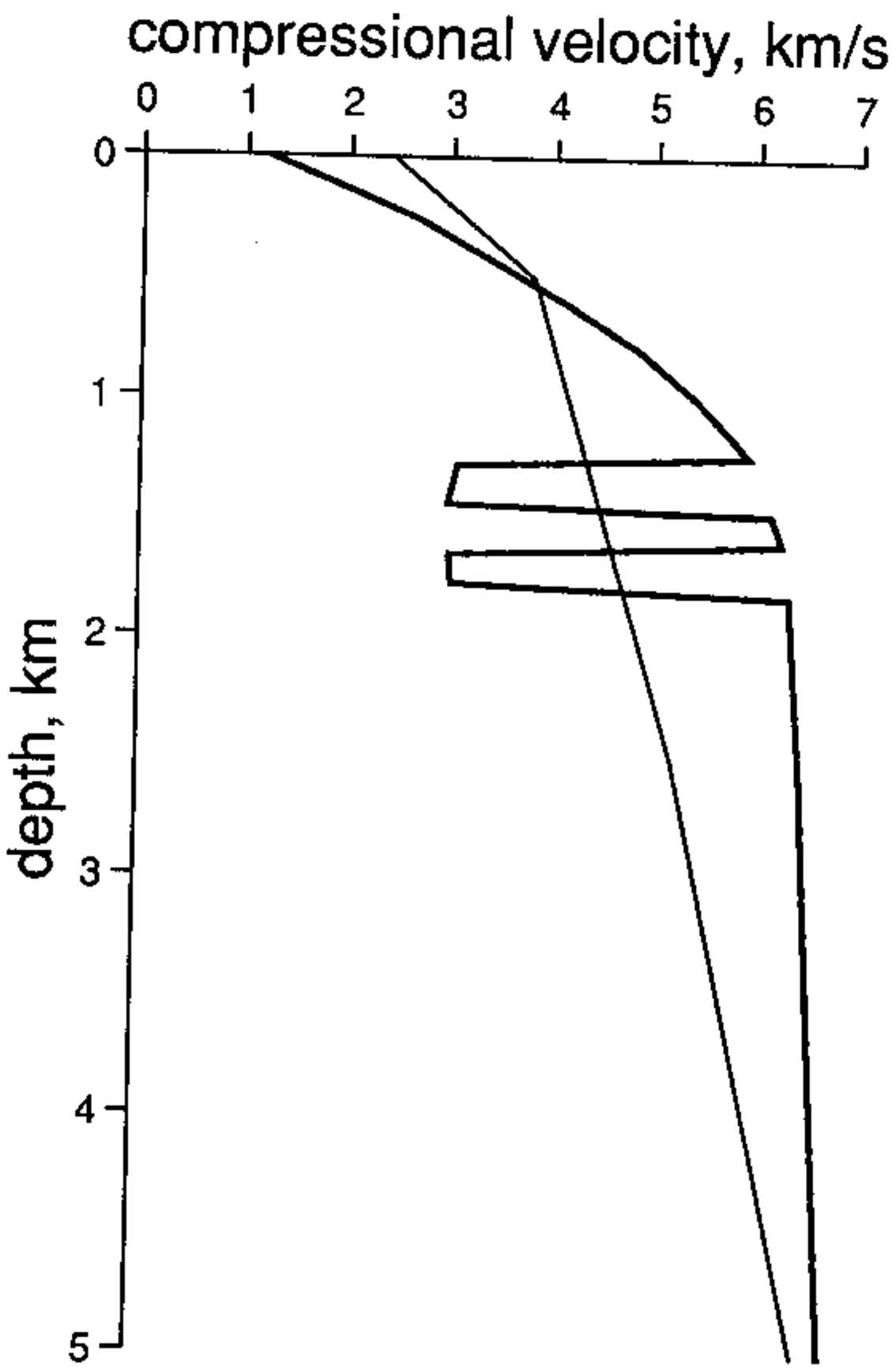

Figure 7

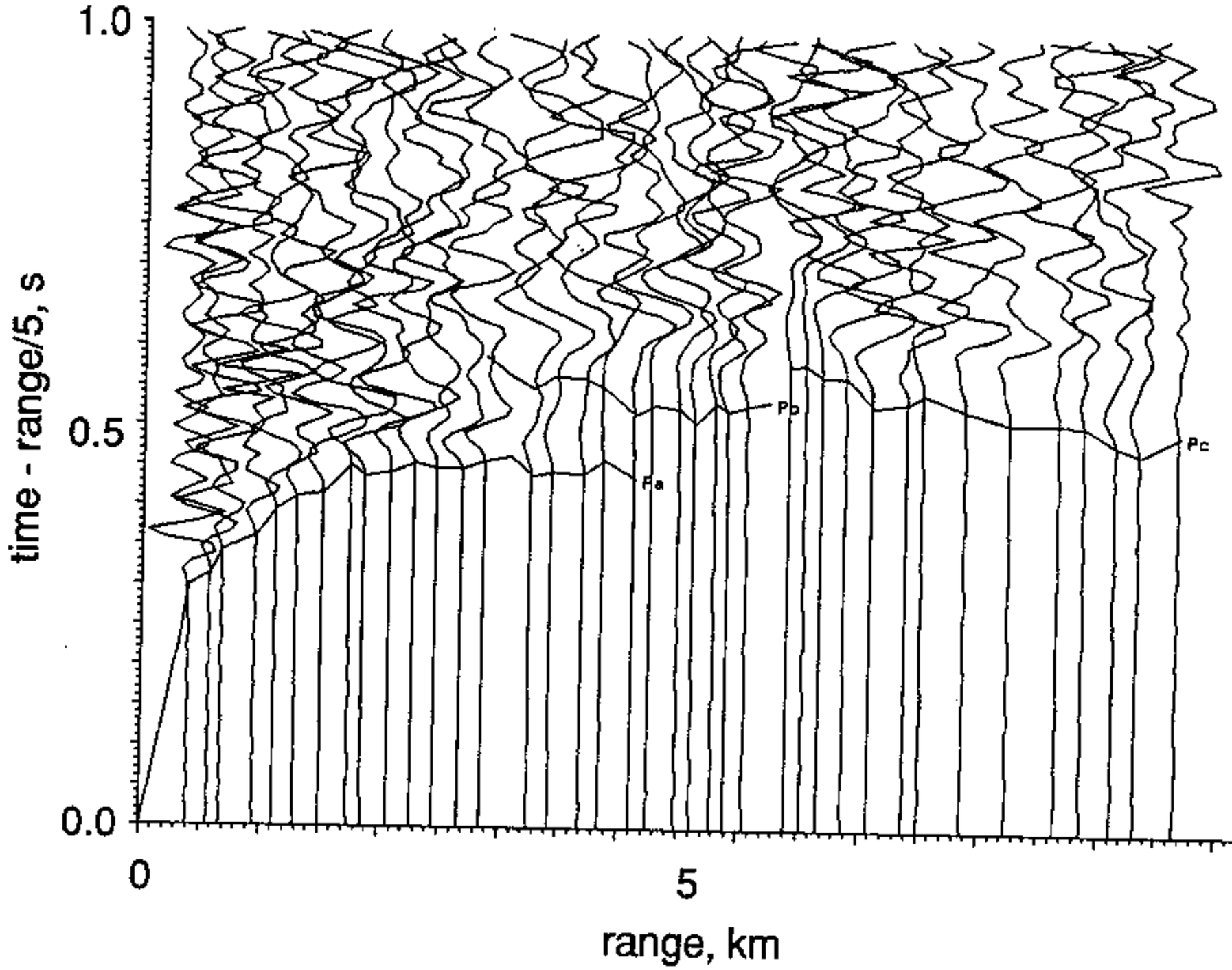

Figure 8

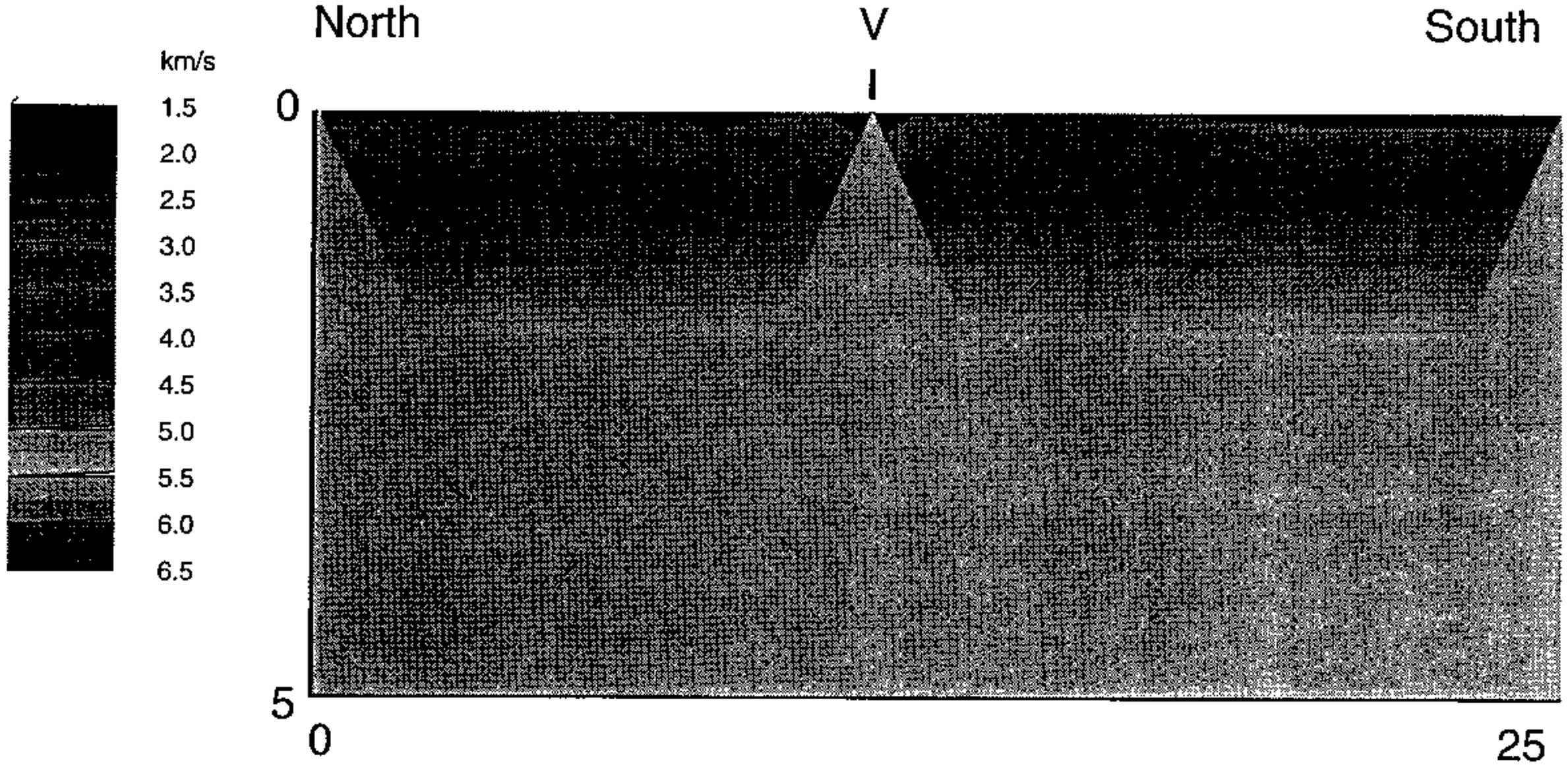

Figure 9

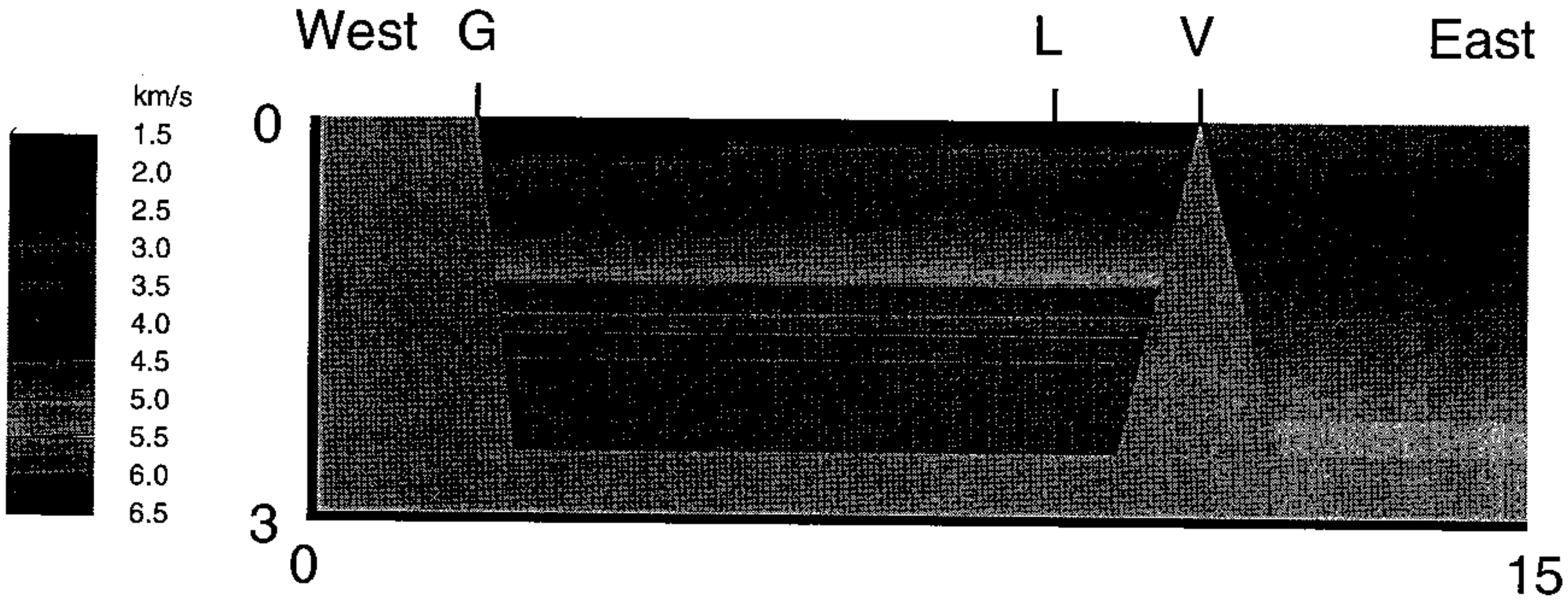

Figure 10

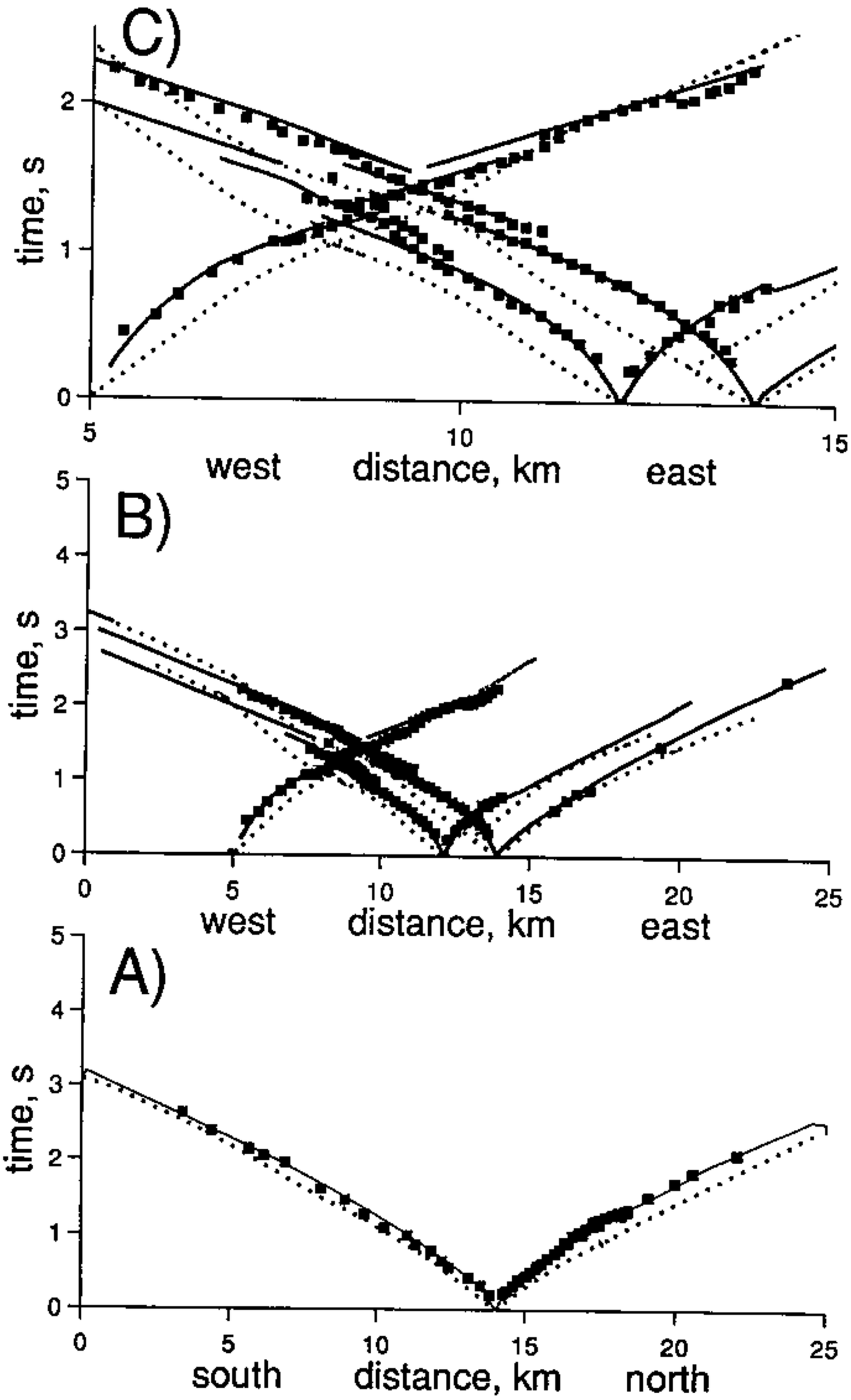
C)
time, s
2
1
0
5
10
15
west
distance, km
east
B)
time, s
5
4
3
2
1
0
0
5
10
15
20
25
west
distance, km
east
A)
time, s
5
4
3
2
1
0
0
5
10
15
20
25
south
distance, km
north

Figure 11

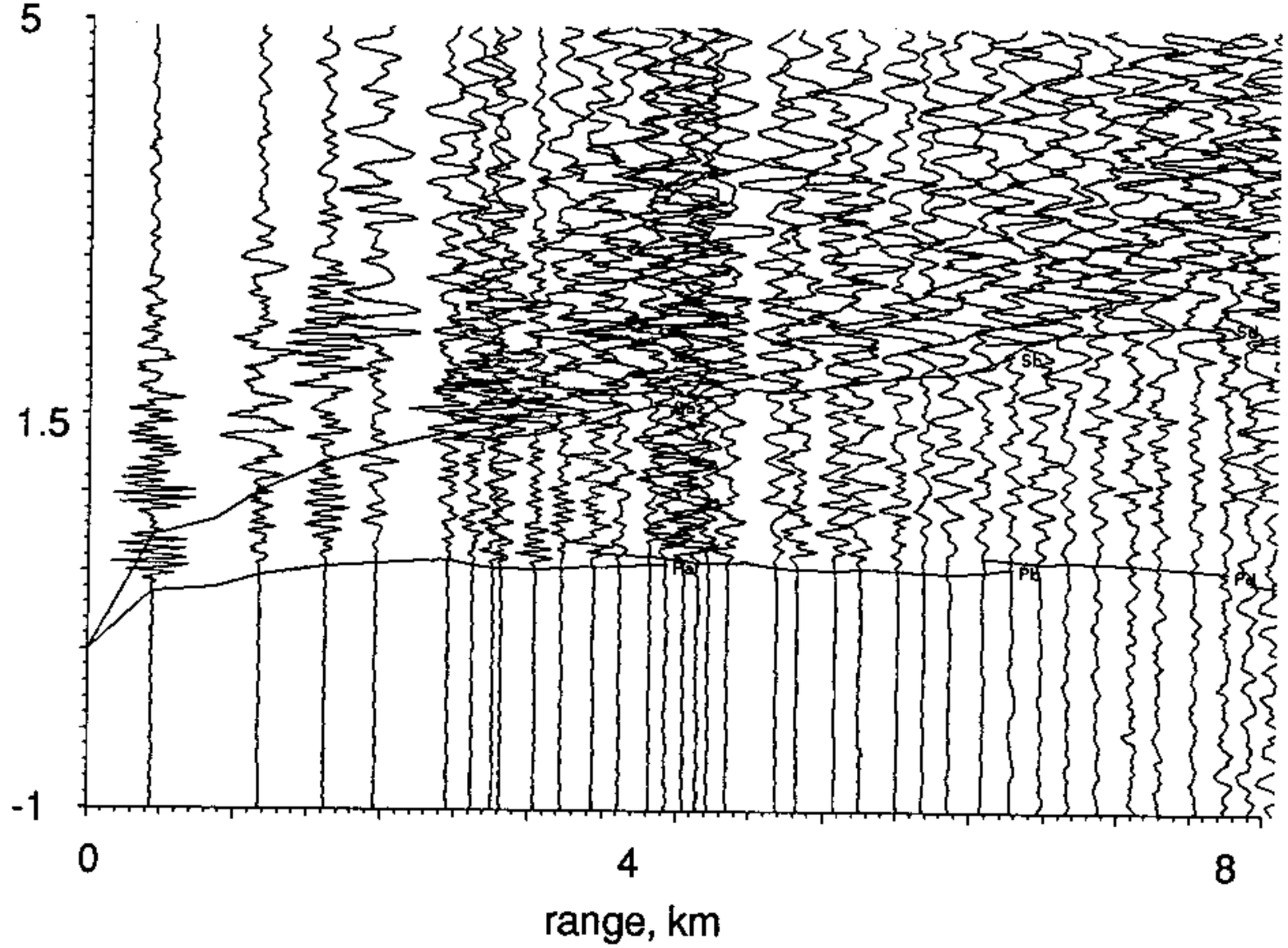

Figure 12

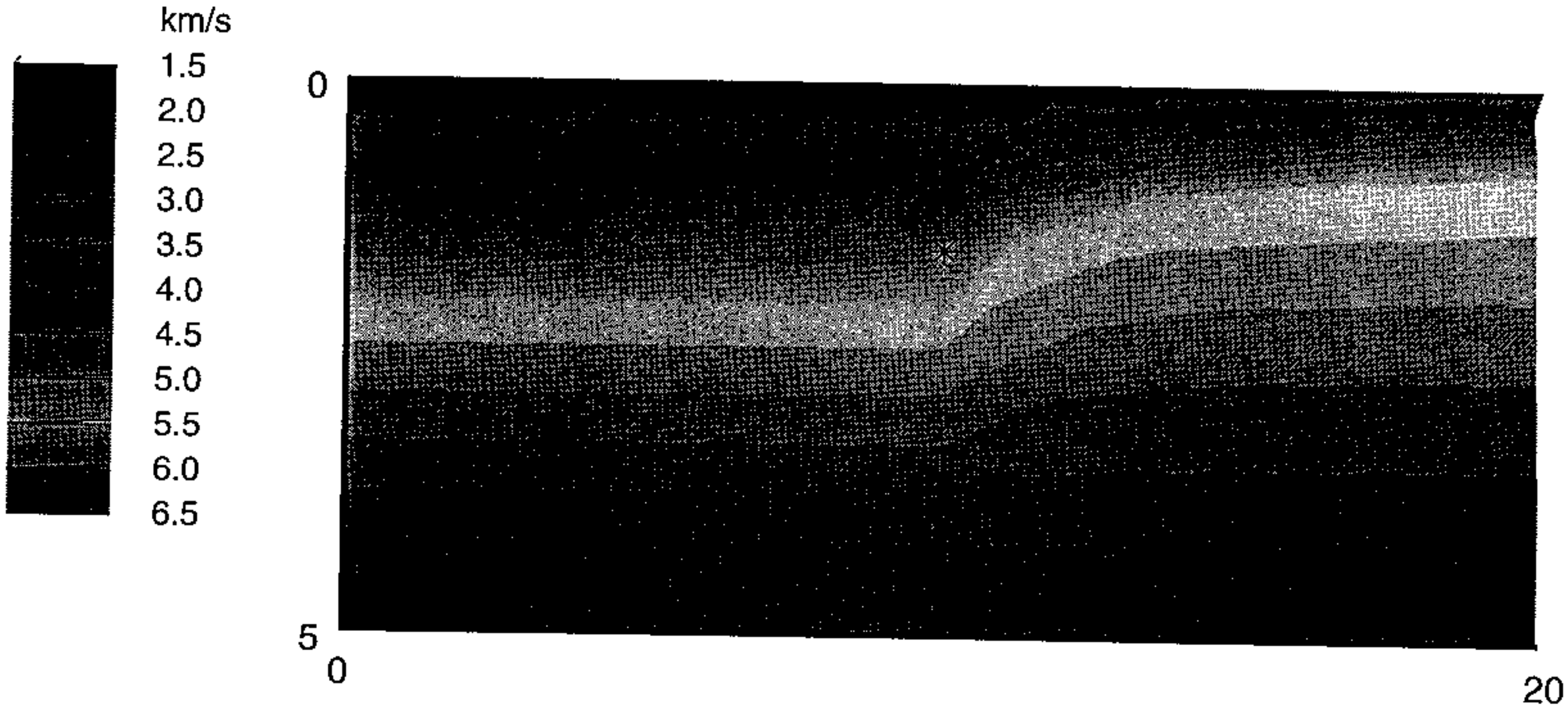

Figure 13

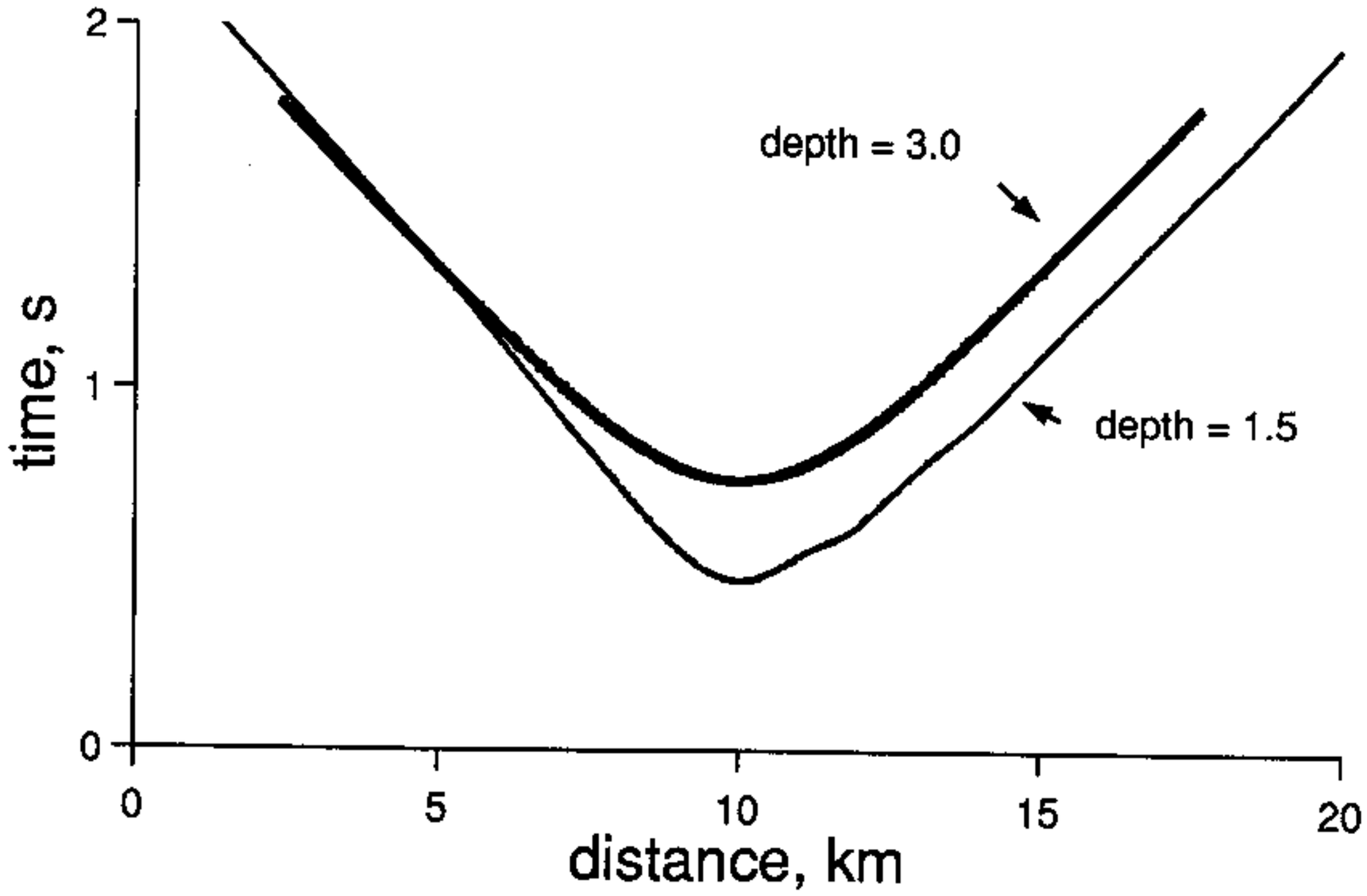

Figure 14

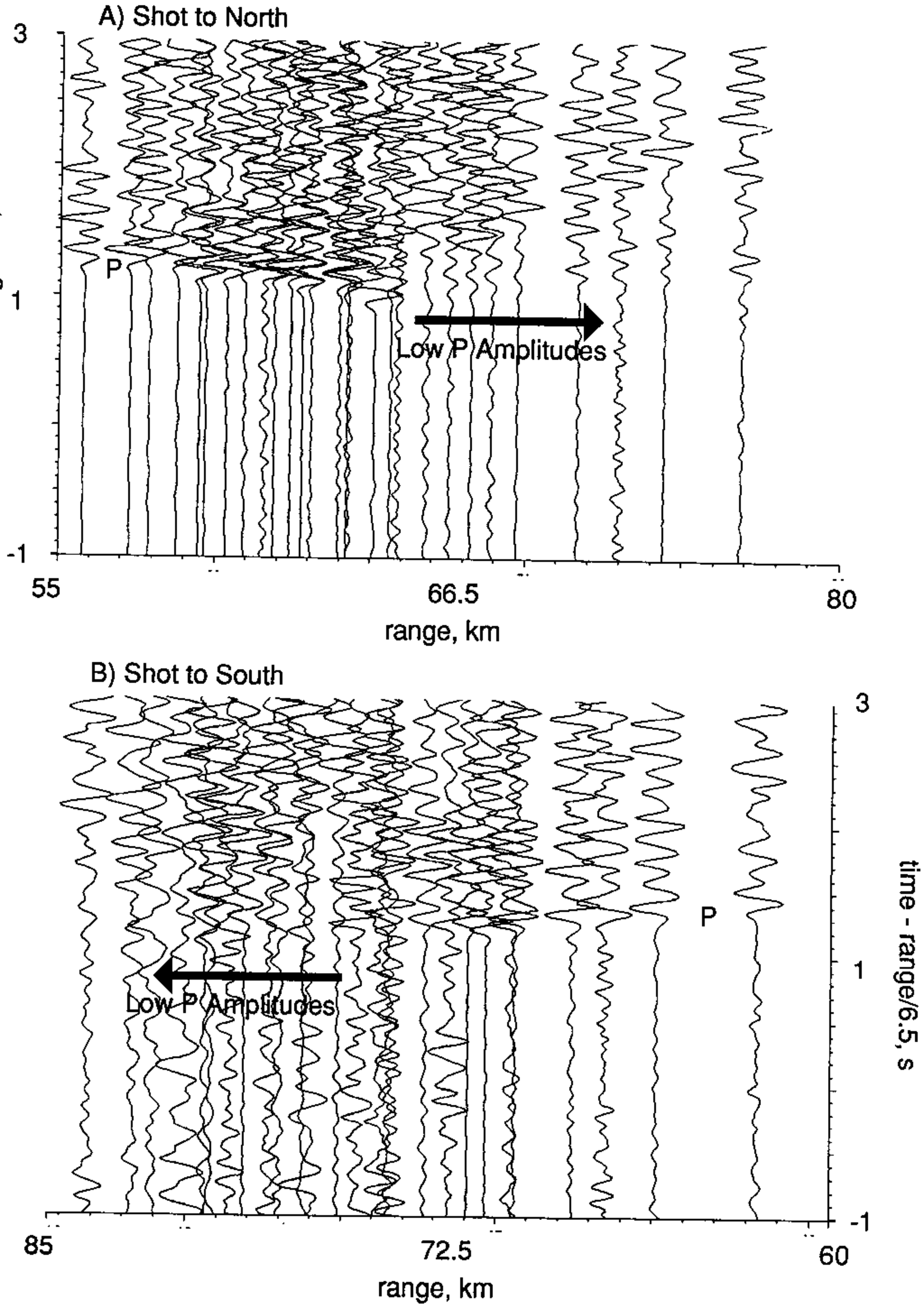
A) Shot to North
3
1
-1
time - range/6.5, s
P
Low P Amplitudes
55
66.5
80
range, km
B) Shot to South
3
1
-1
time - range/6.5, s
P
Low P Amplitudes
85
72.5
60
range, km

Figure 15

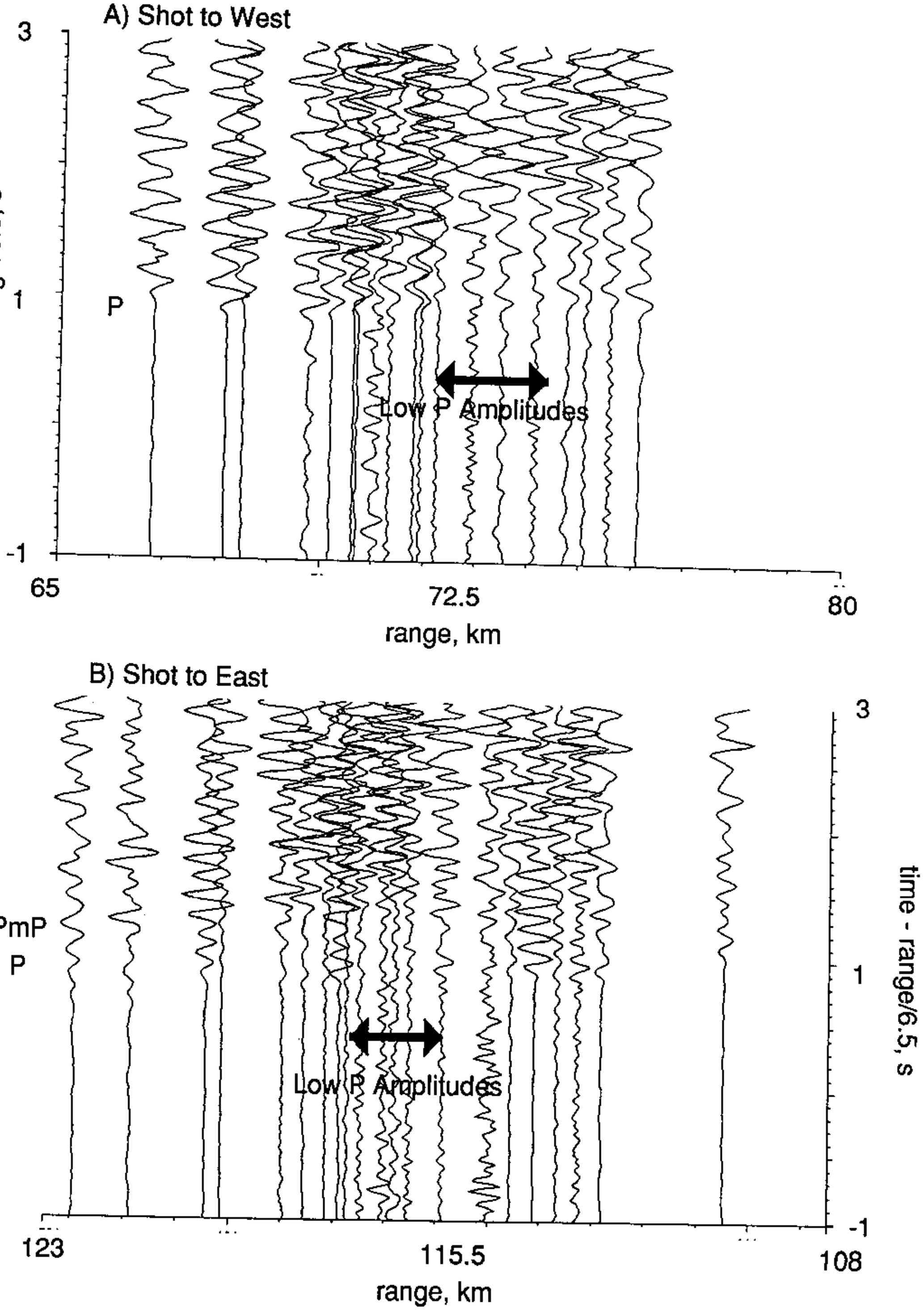
A) Shot to West
3
1
-1
time - range/6.5, s
P
Low P Amplitudes
65
72.5
80
range, km
B) Shot to East
PmP
P
3
1
-1
time - range/6.5, s
Low P Amplitudes
123
115.5
108
range, km

Figure 16

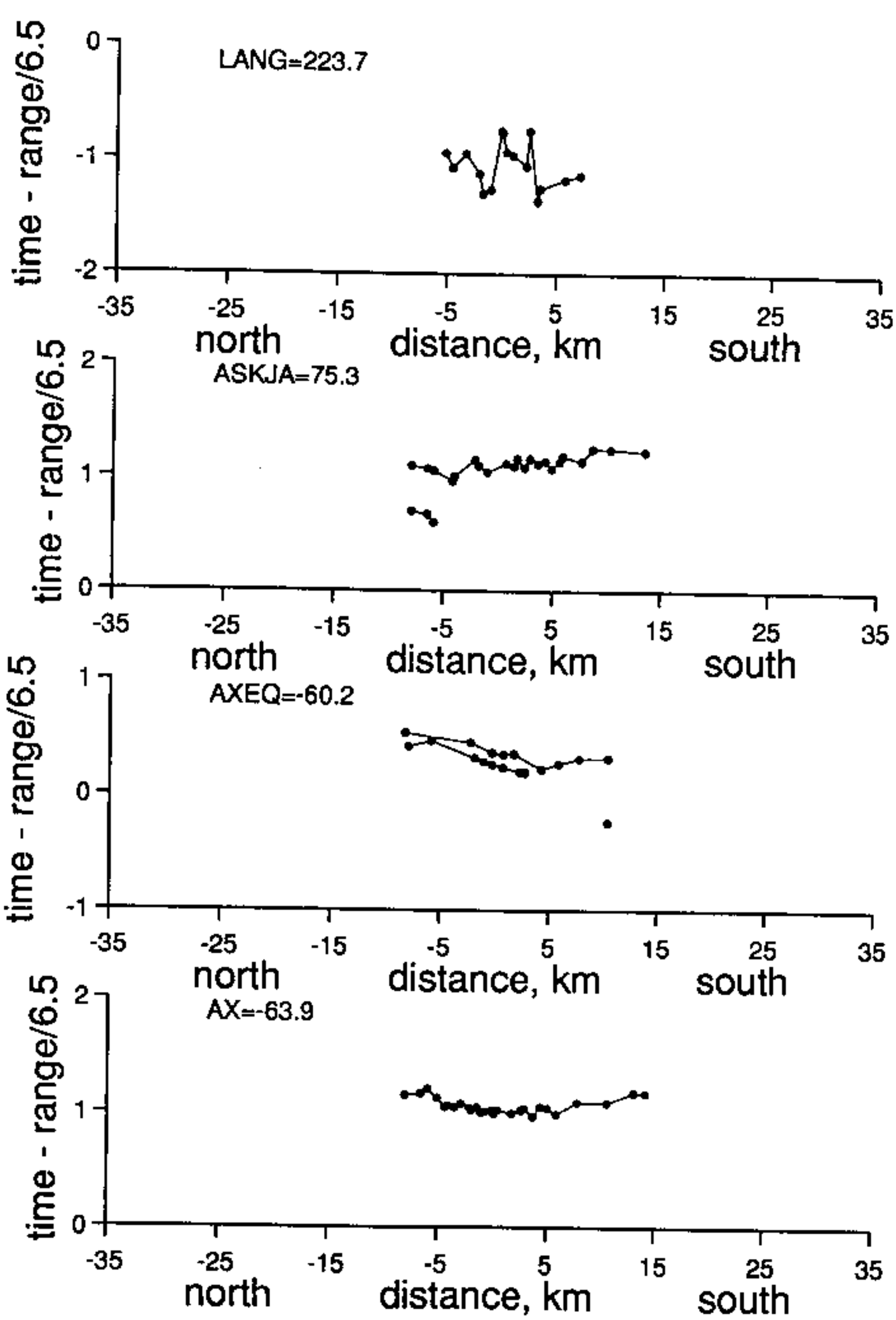
time - range/6.5
LANG=223.7
north
distance, km
south
ASKJA=75.3
AXEQ=-60.2
AX=-63.9

Figure 17

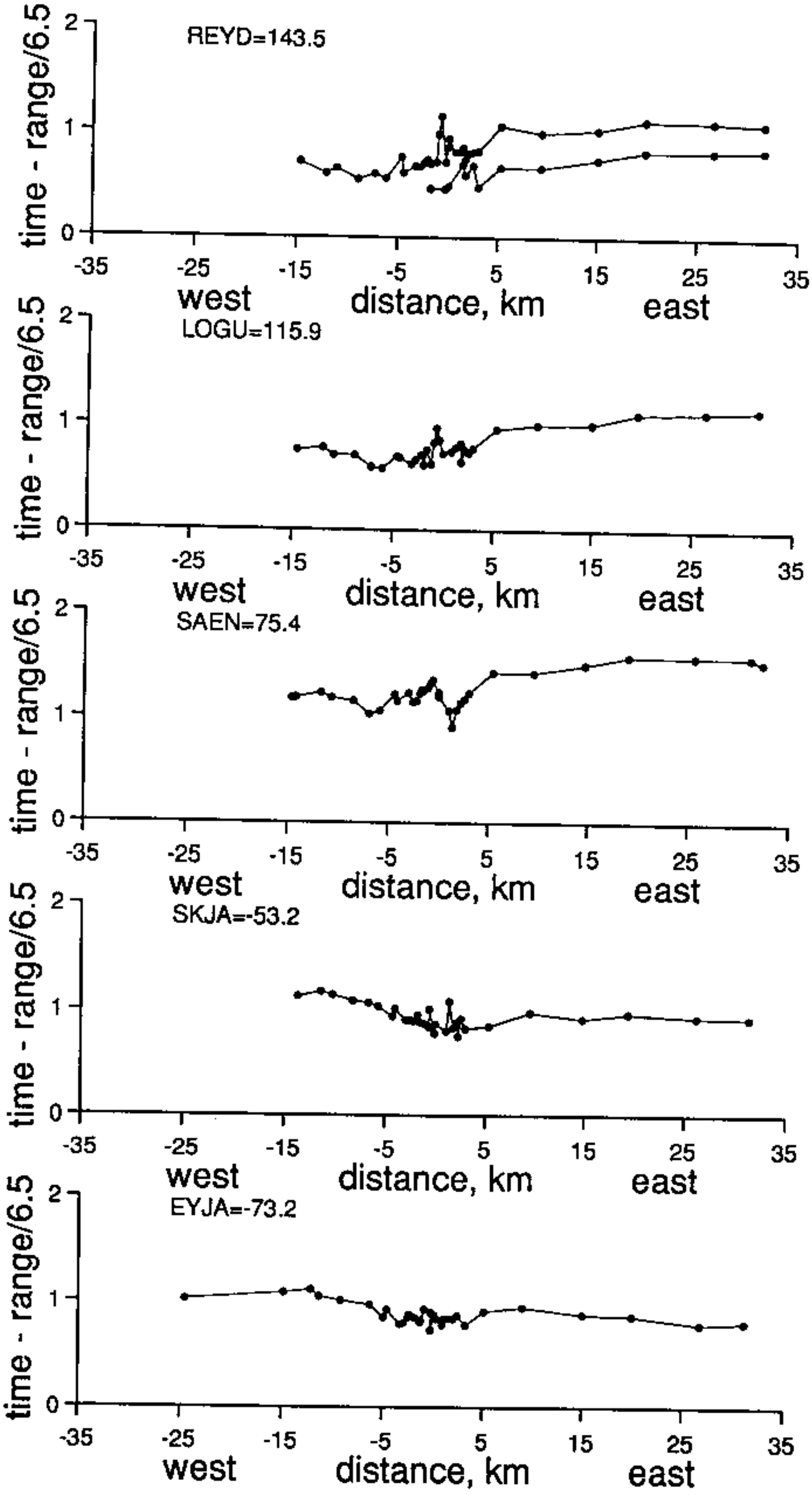
REYD=143.5
LOGU=115.9
SAEN=75.4
SKJA=-53.2
EYJA=-73.2
time - range/6.5
2
1
0
-35
-25
-15
-5
5
15
25
35
west
distance, km
east

Figure 18

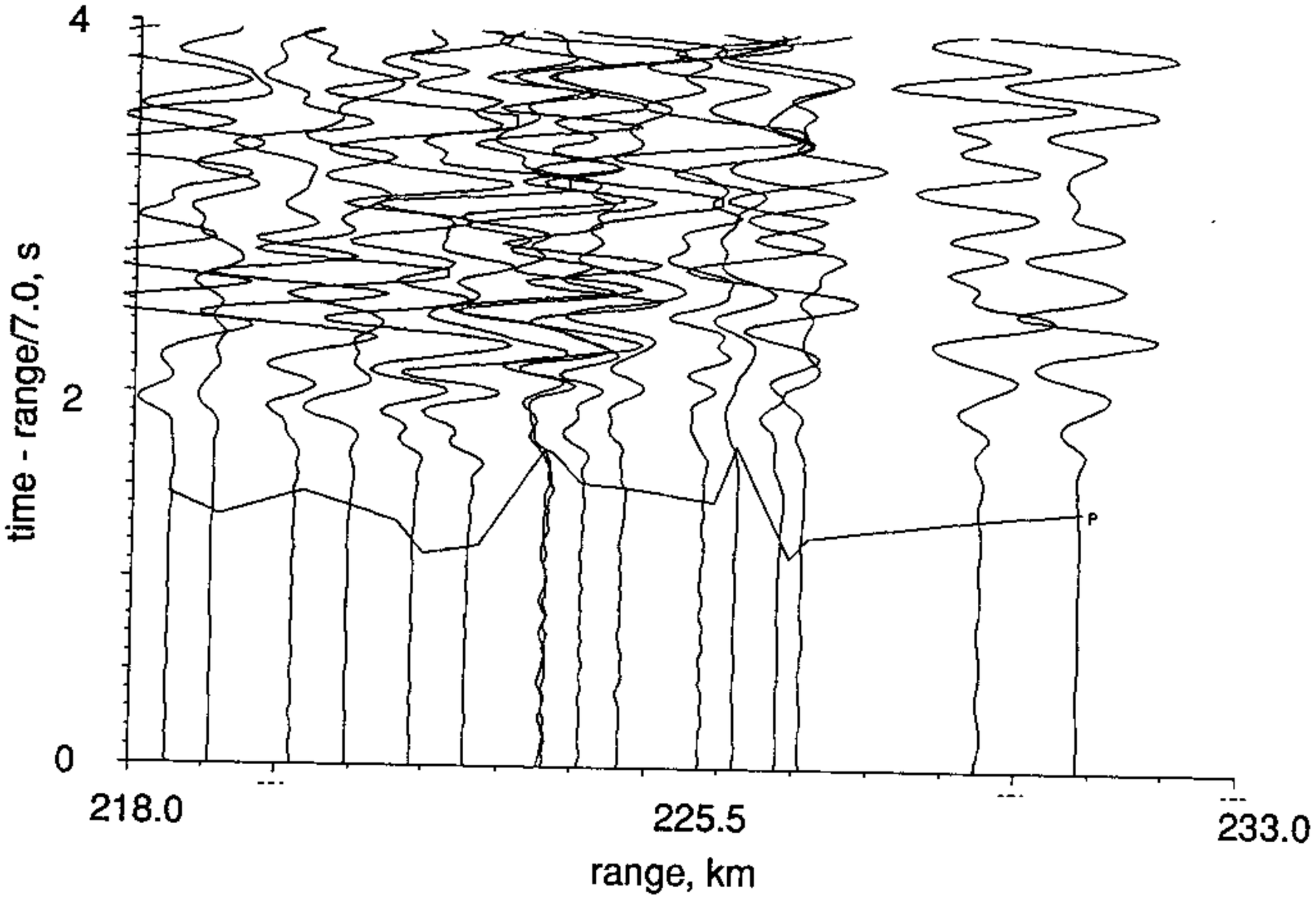

Figure 19

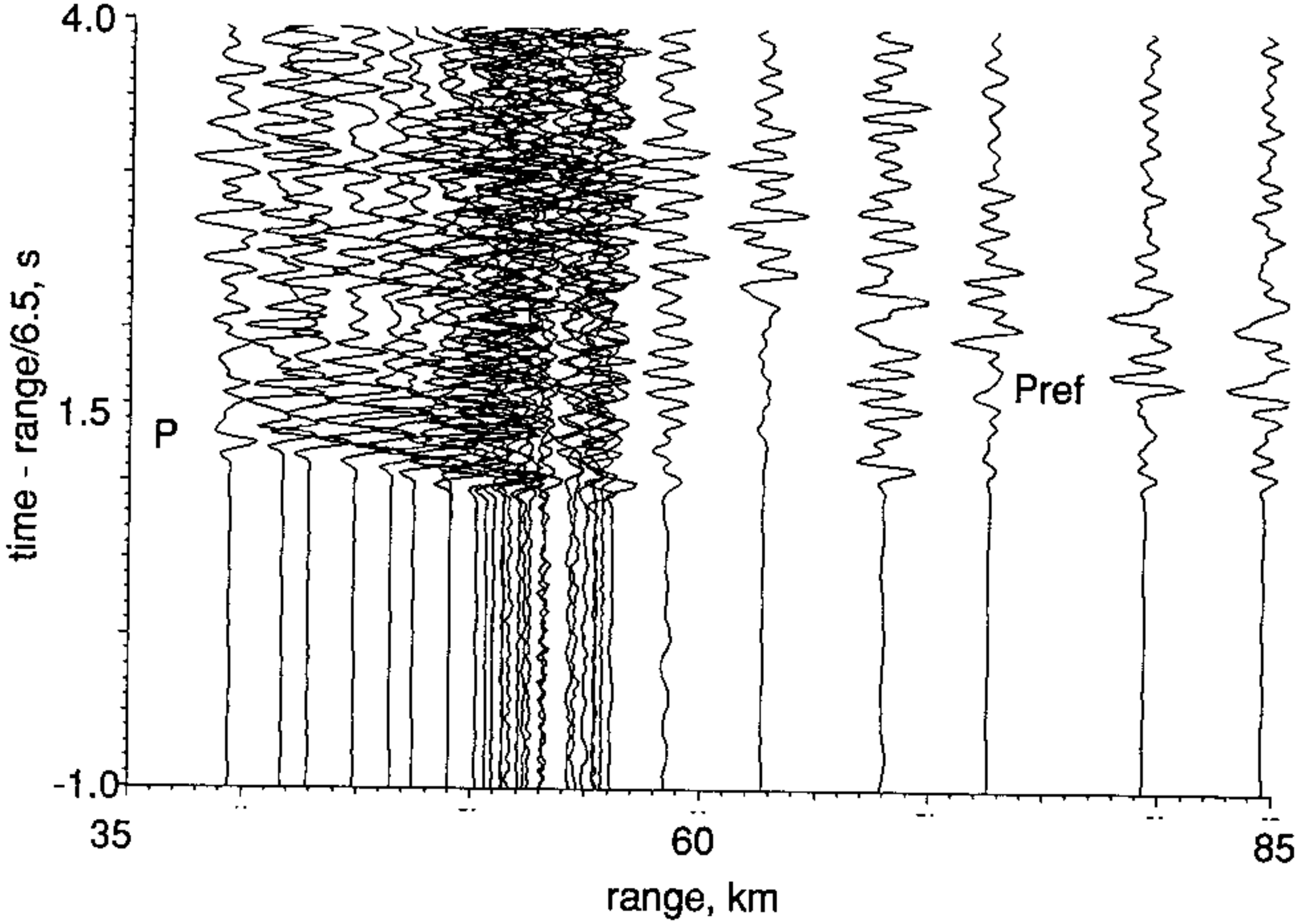

Figure 20

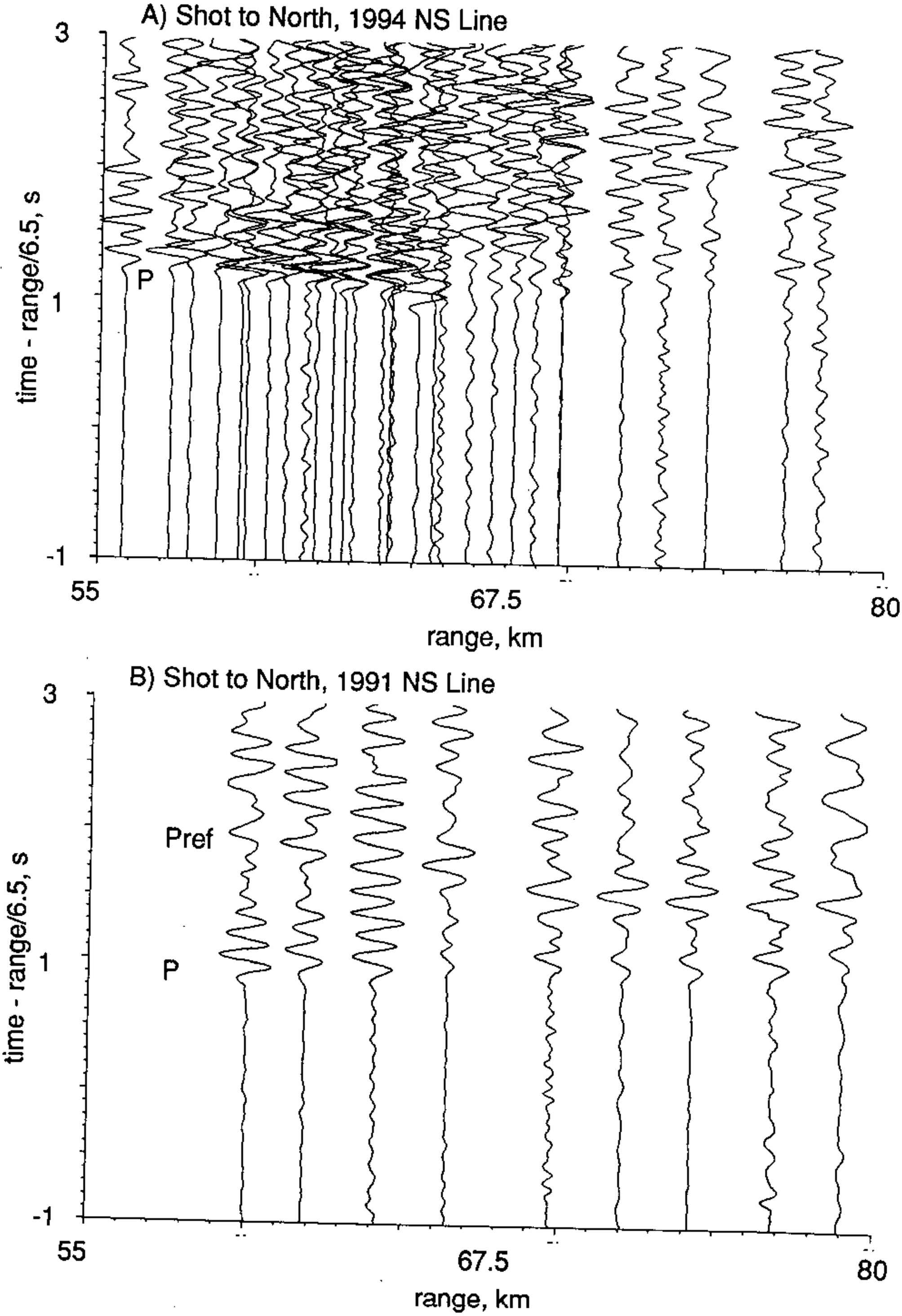
A) Shot to North, 1994 NS Line
3
1
-1
P
time - range/6.5, s
55
67.5
80
range, km
B) Shot to North, 1991 NS Line
3
Pref
P
1
-1
time - range/6.5, s
55
67.5
80
range, km

Figure 21

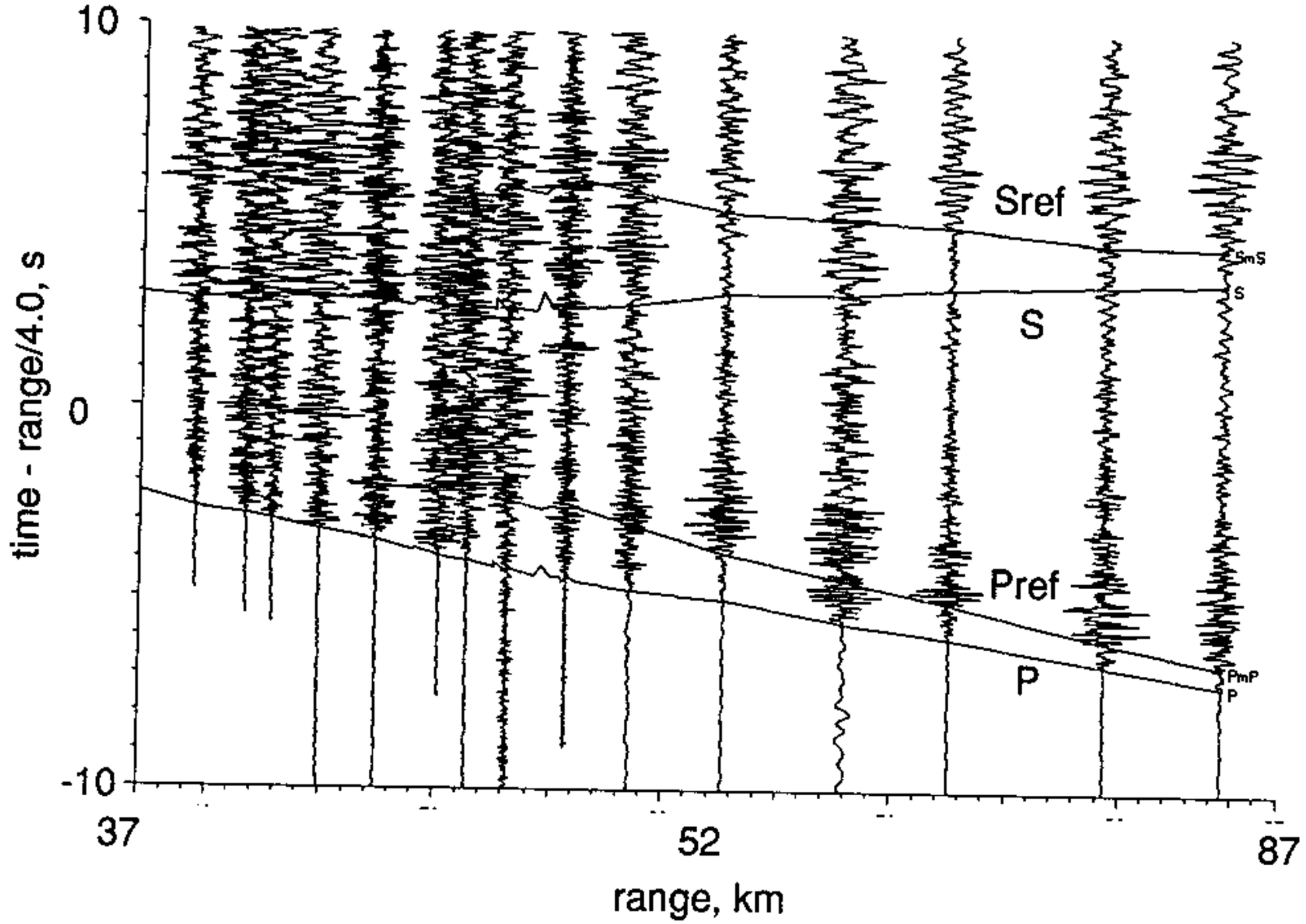

Figure 22

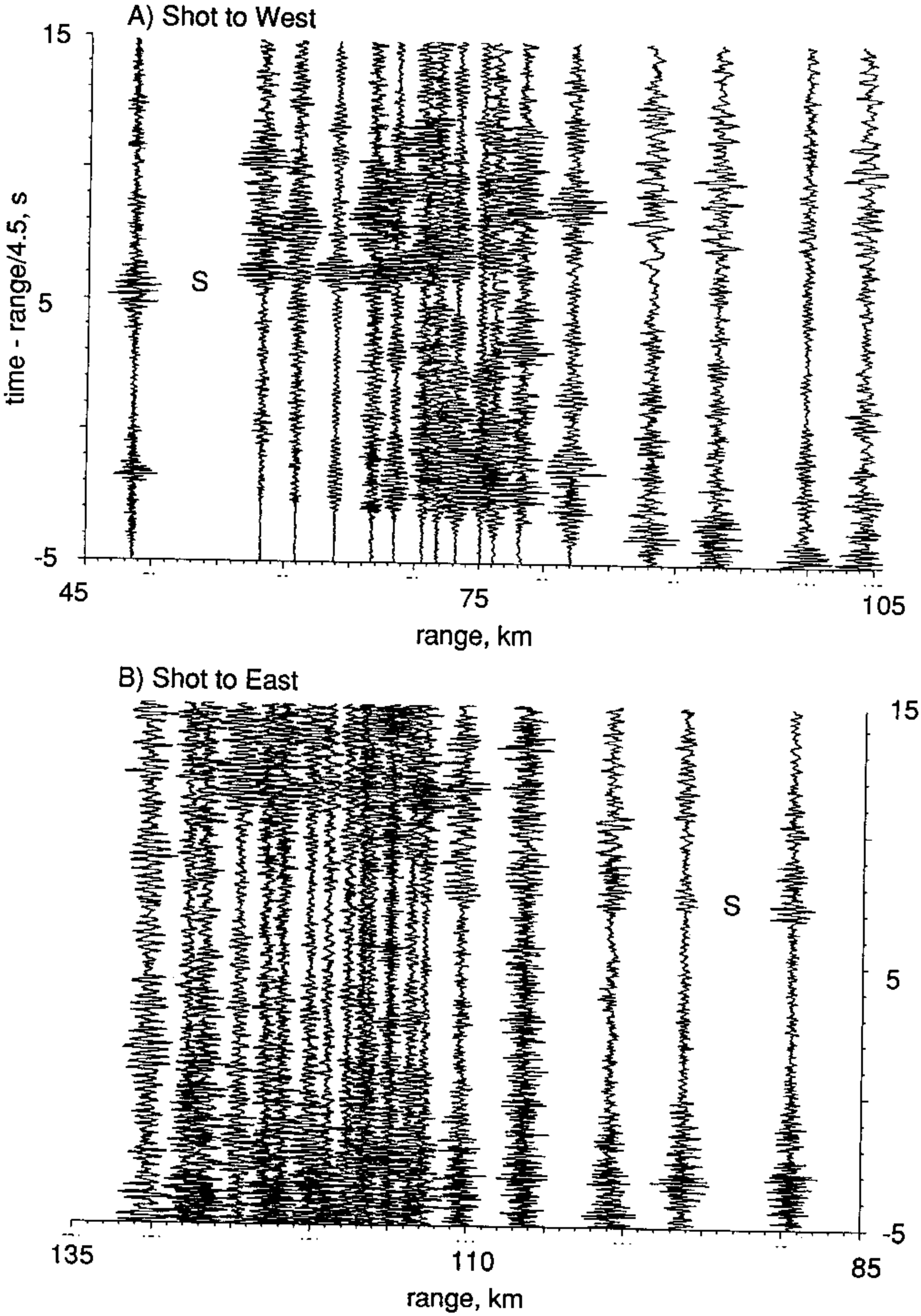
A) Shot to West
15
5
-5
time - range/4.5, s
S
45
75
105
range, km
B) Shot to East
15
5
-5
time - range/4.5, s
S
135
110
85
range, km

Figure 23

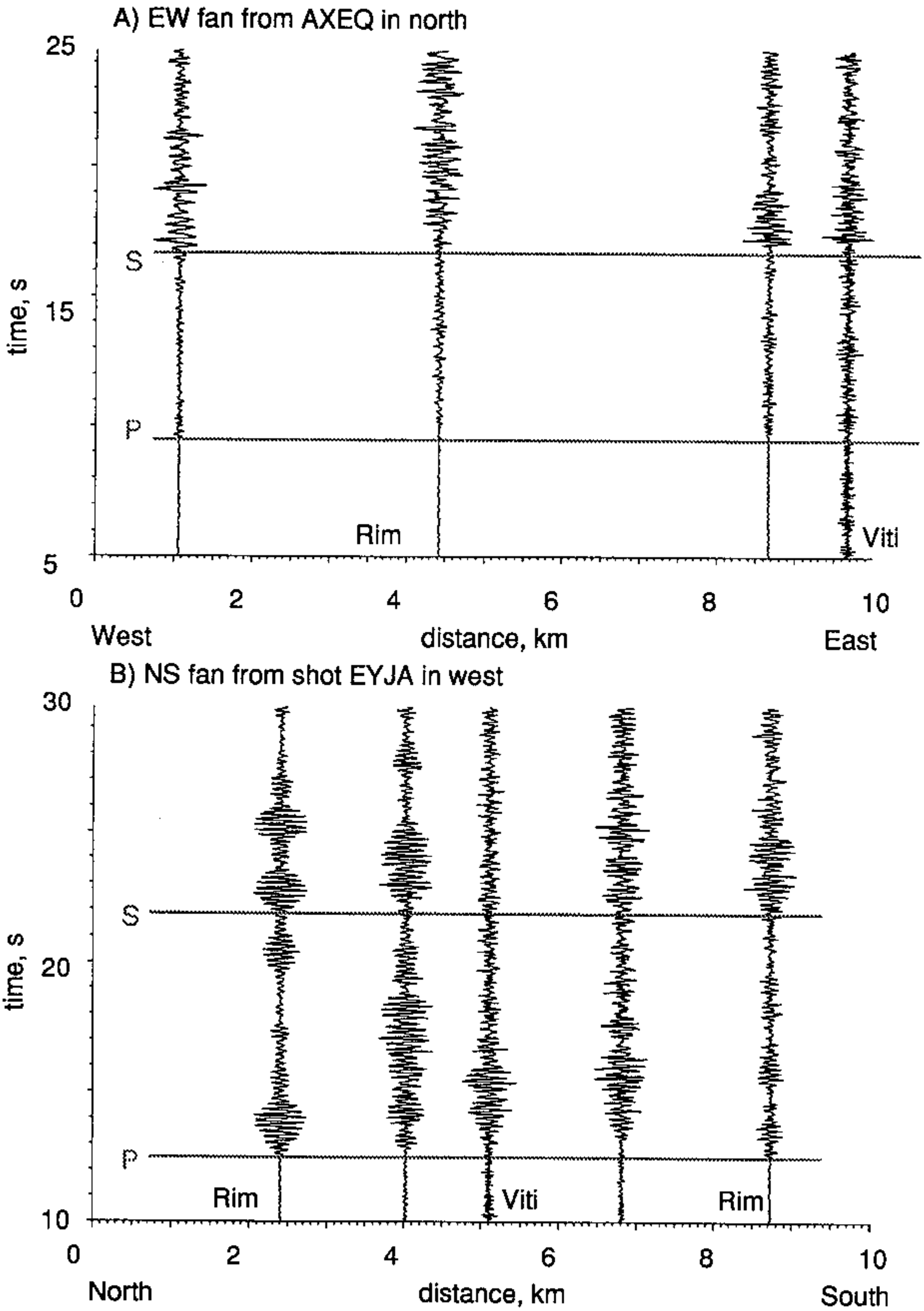
A) EW fan from AXEQ in north
25
15
5
time, s
S
P
Rim
Viti
0
2
4
6
8
10
West
distance, km
East
B) NS fan from shot EYJA in west
30
20
10
time, s
S
P
Rim
Viti
Rim
0
2
4
6
8
10
North
distance, km
South

Figure 24

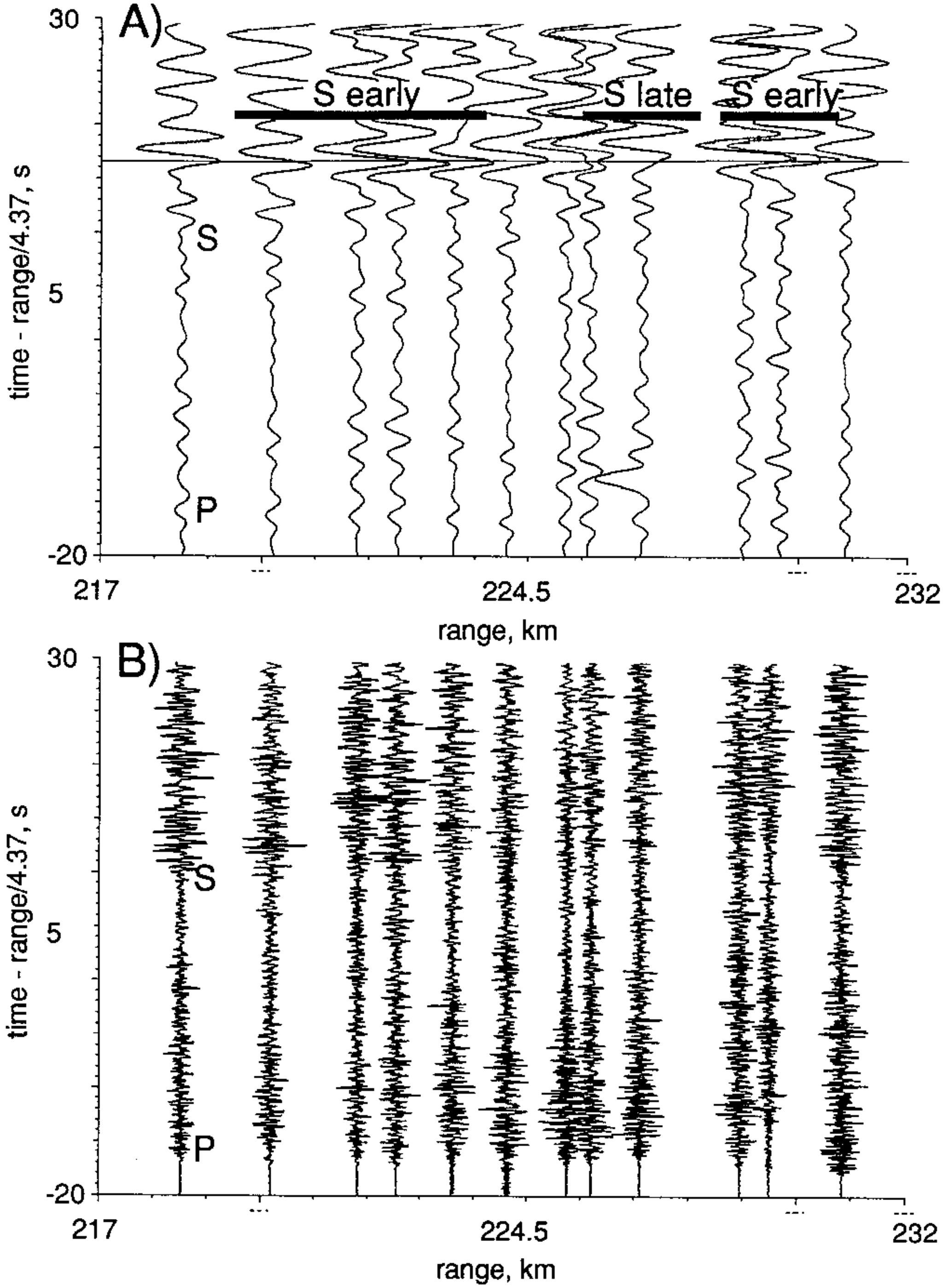
A)
30
S early
S late
S early
S
P
5
-20
217
224.5
232
range, km
time - range/4.37, s
B)
30
S
P
5
-20
217
224.5
232
range, km
time - range/4.37, s

Figure 25

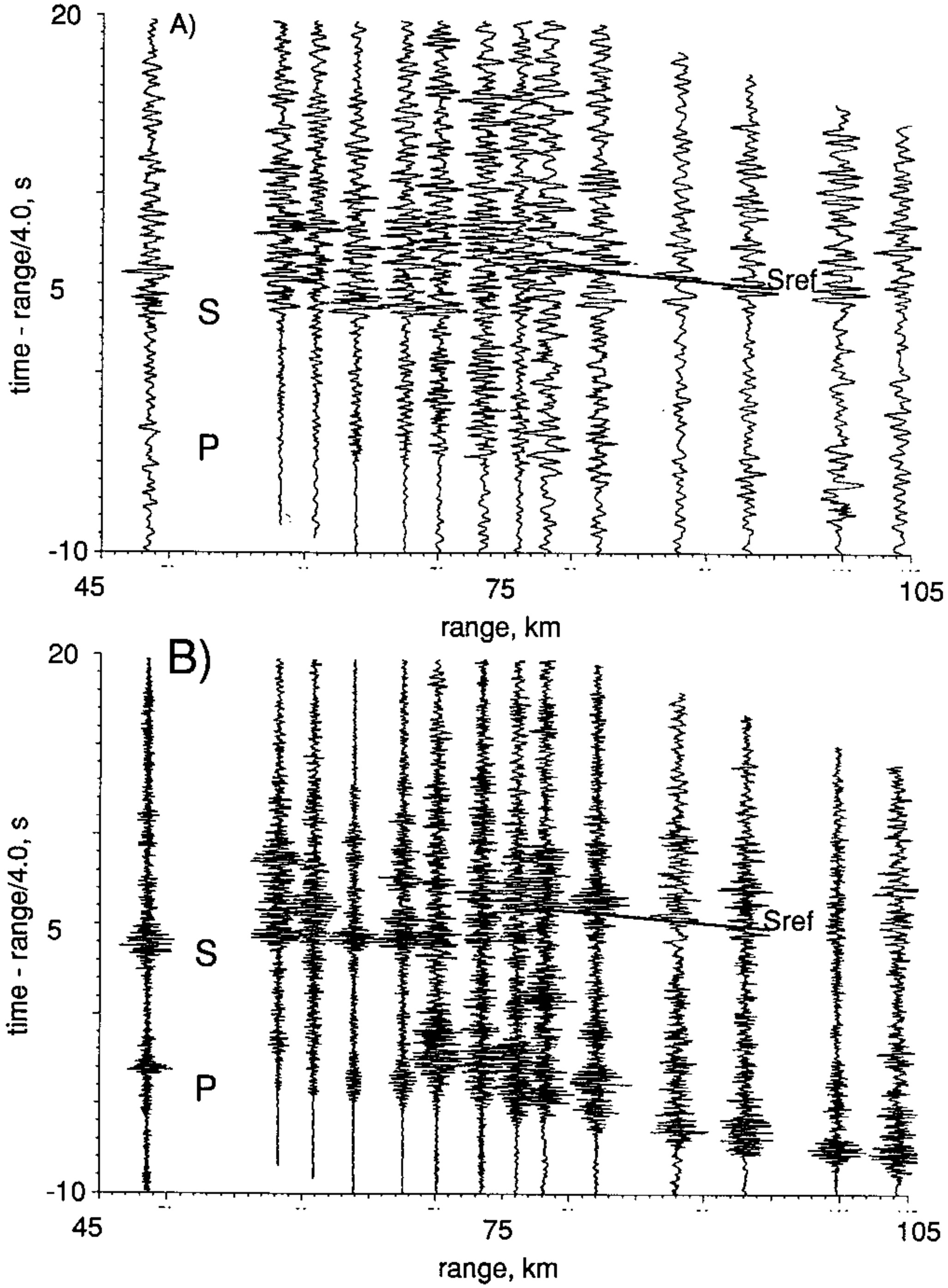

Figure 26

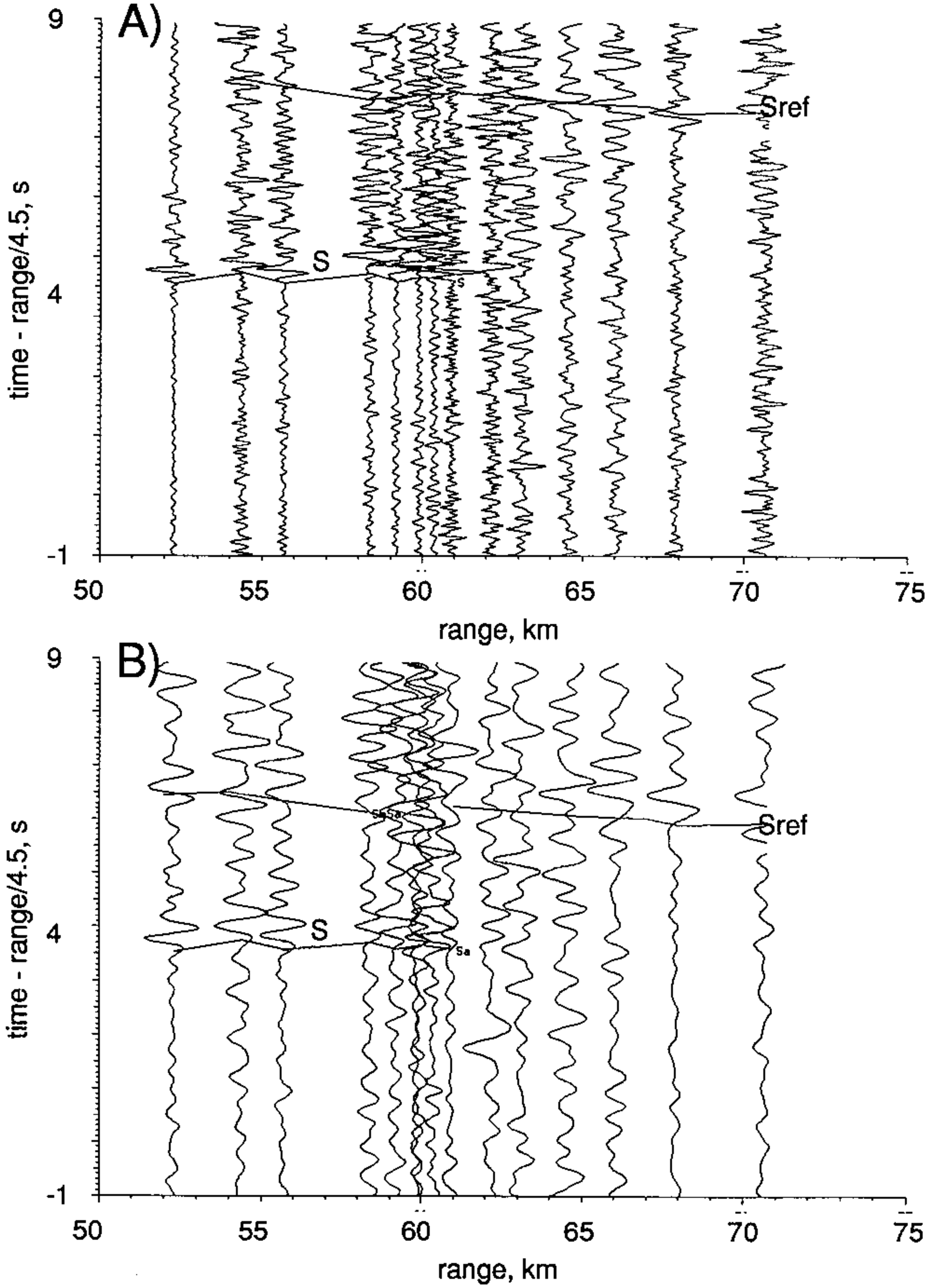
A)
time - range/4.5, s
9
4
-1
50
55
60
65
70
75
range, km
S
Sref
B)
time - range/4.5, s
9
4
-1
50
55
60
65
70
75
range, km
S
Sa
Sref

Figure 27

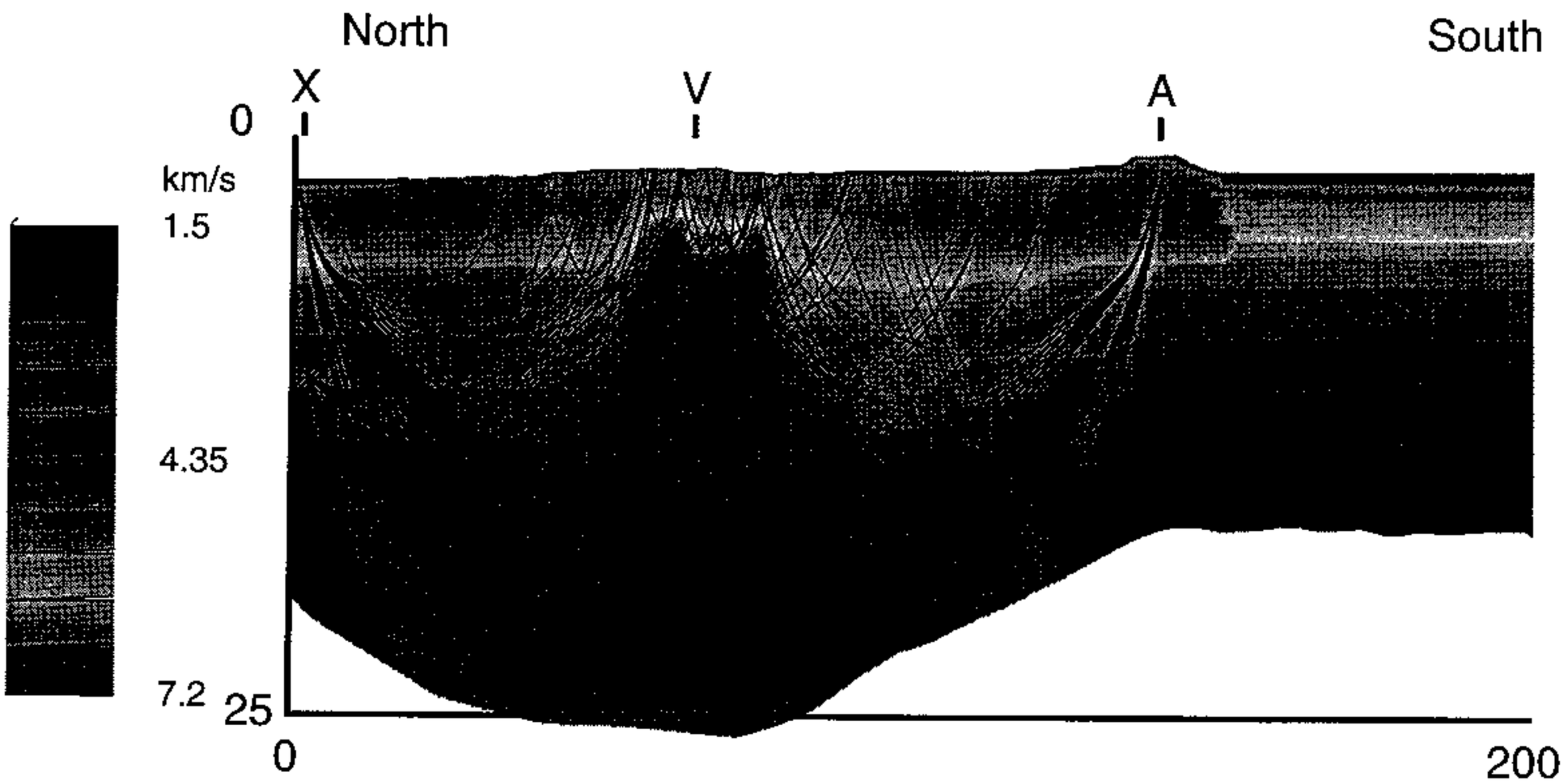

Figure 28

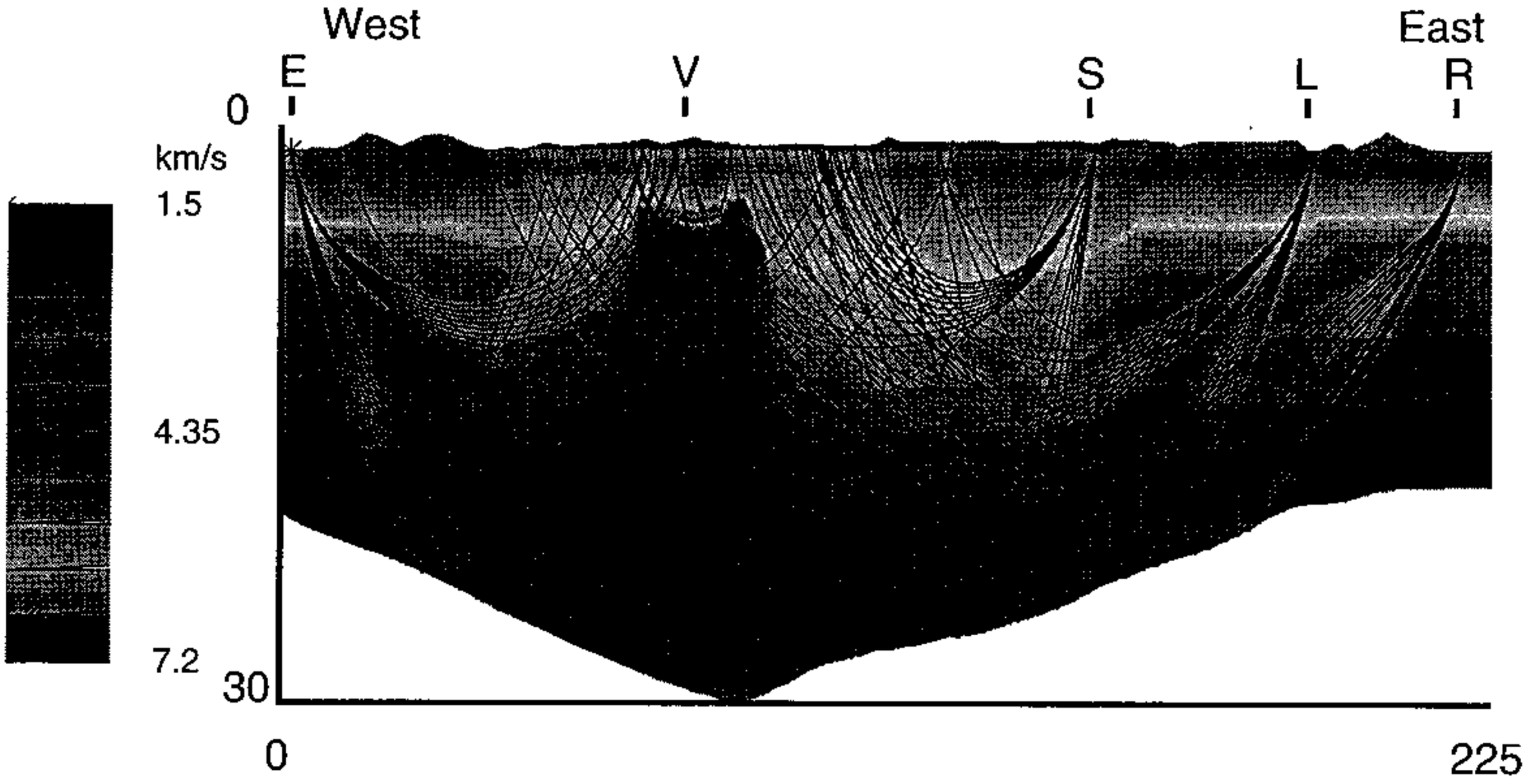

Figure 29

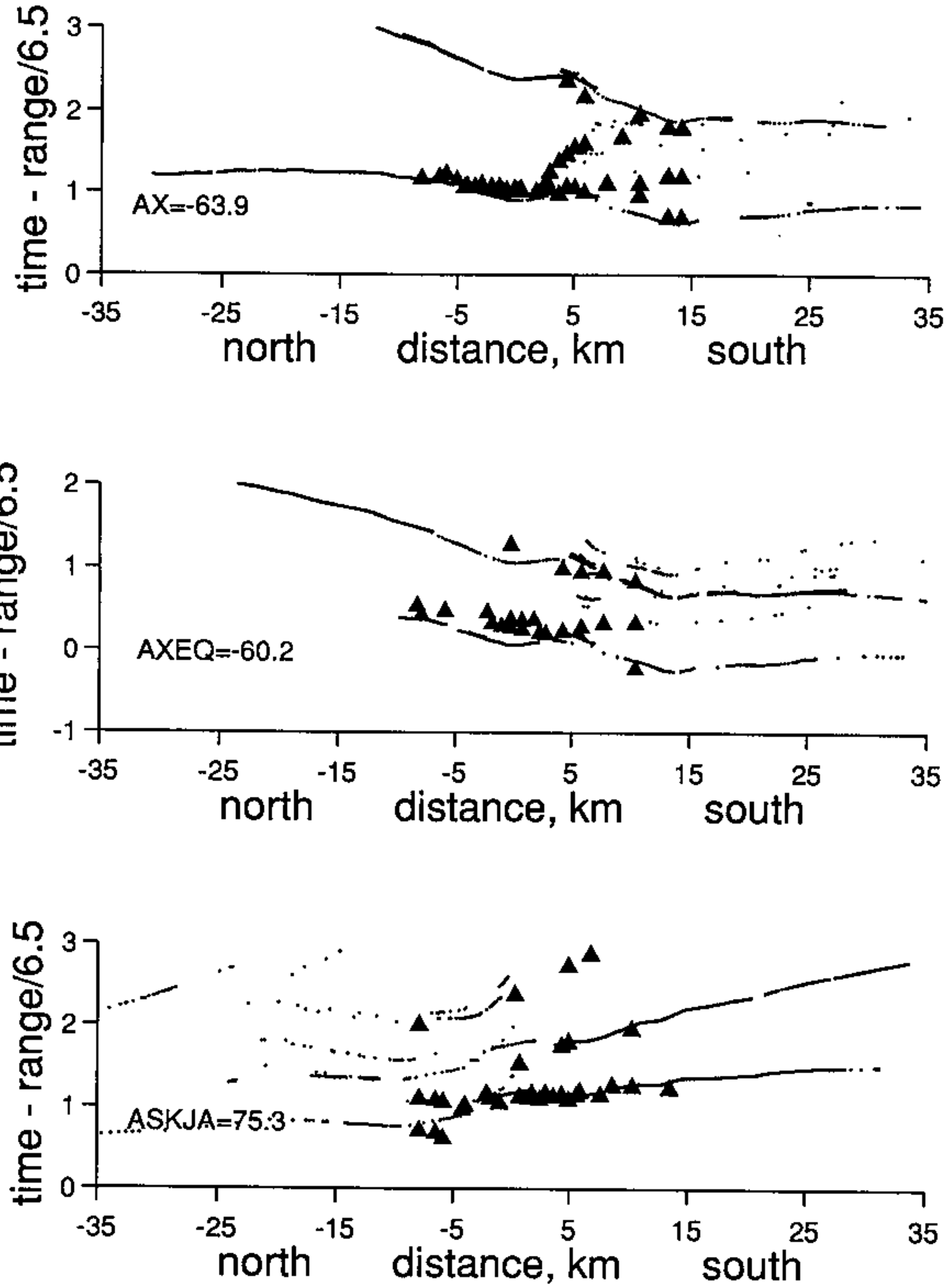
time - range/6.5
3
2
1
0
AX=-63.9
-35
-25
-15
-5
5
15
25
35
north
distance, km
south
time - range/6.5
2
1
0
-1
AXEQ=-60.2
-35
-25
-15
-5
5
15
25
35
north
distance, km
south
time - range/6.5
3
2
1
0
ASKJA=75.3
-35
-25
-15
-5
5
15
25
35
north
distance, km
south

Figure 30

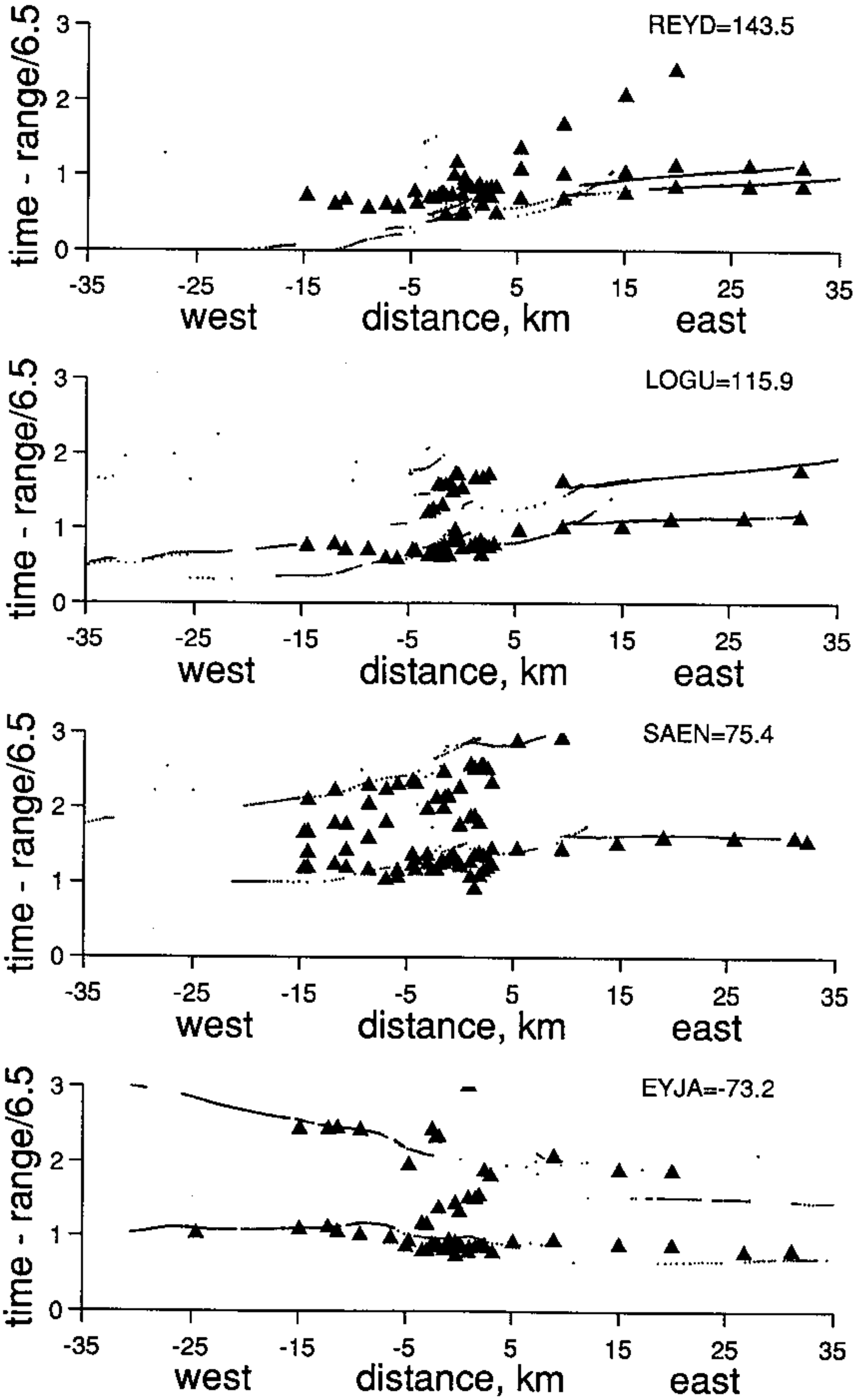
REYD=143.5
LOGU=115.9
SAEN=75.4
EYJA=-73.2
time - range/6.5
0
1
2
3
-35
-25
-15
-5
5
15
25
35
west
distance, km
east

Figure 31

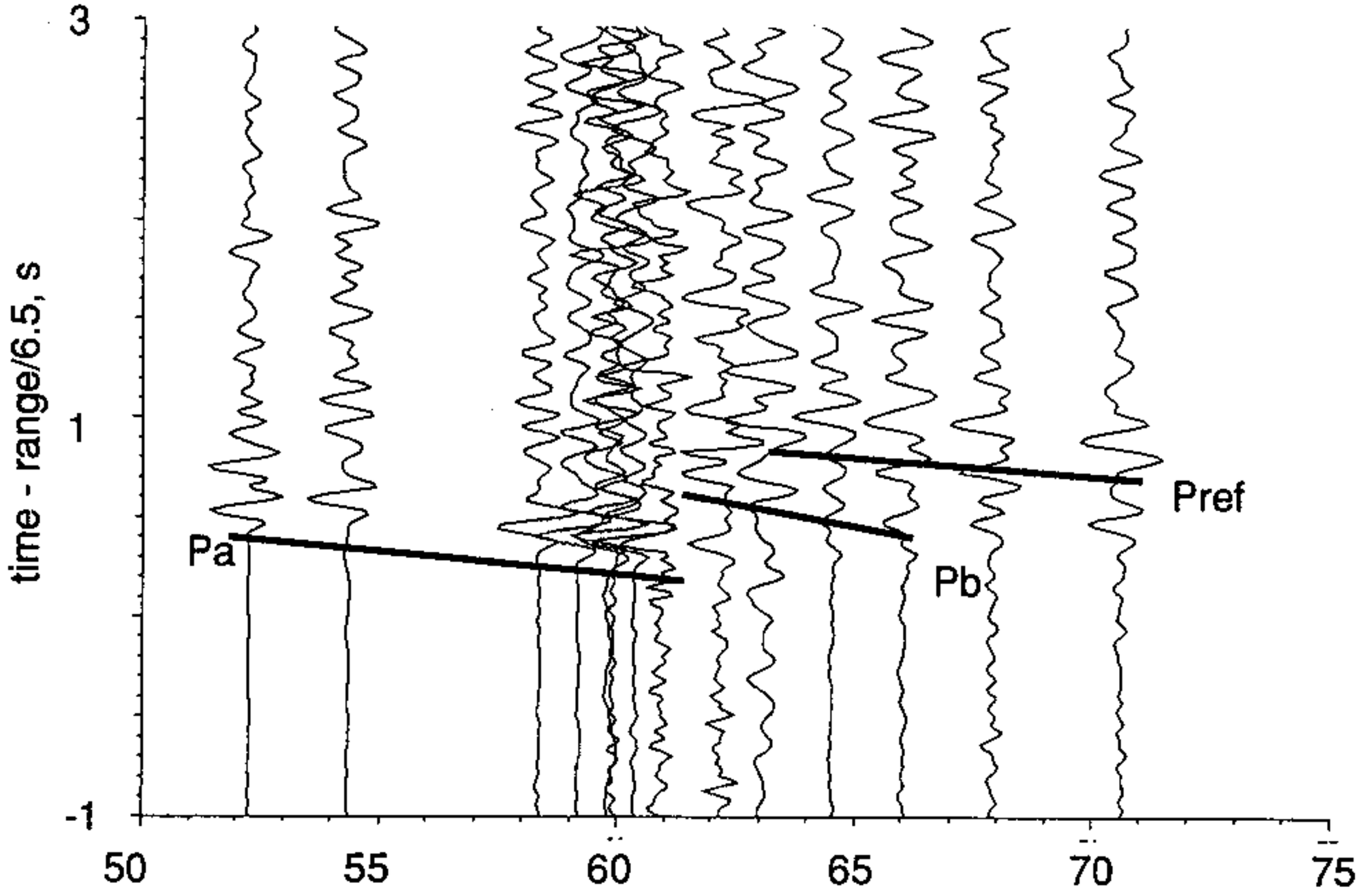

Figure 32

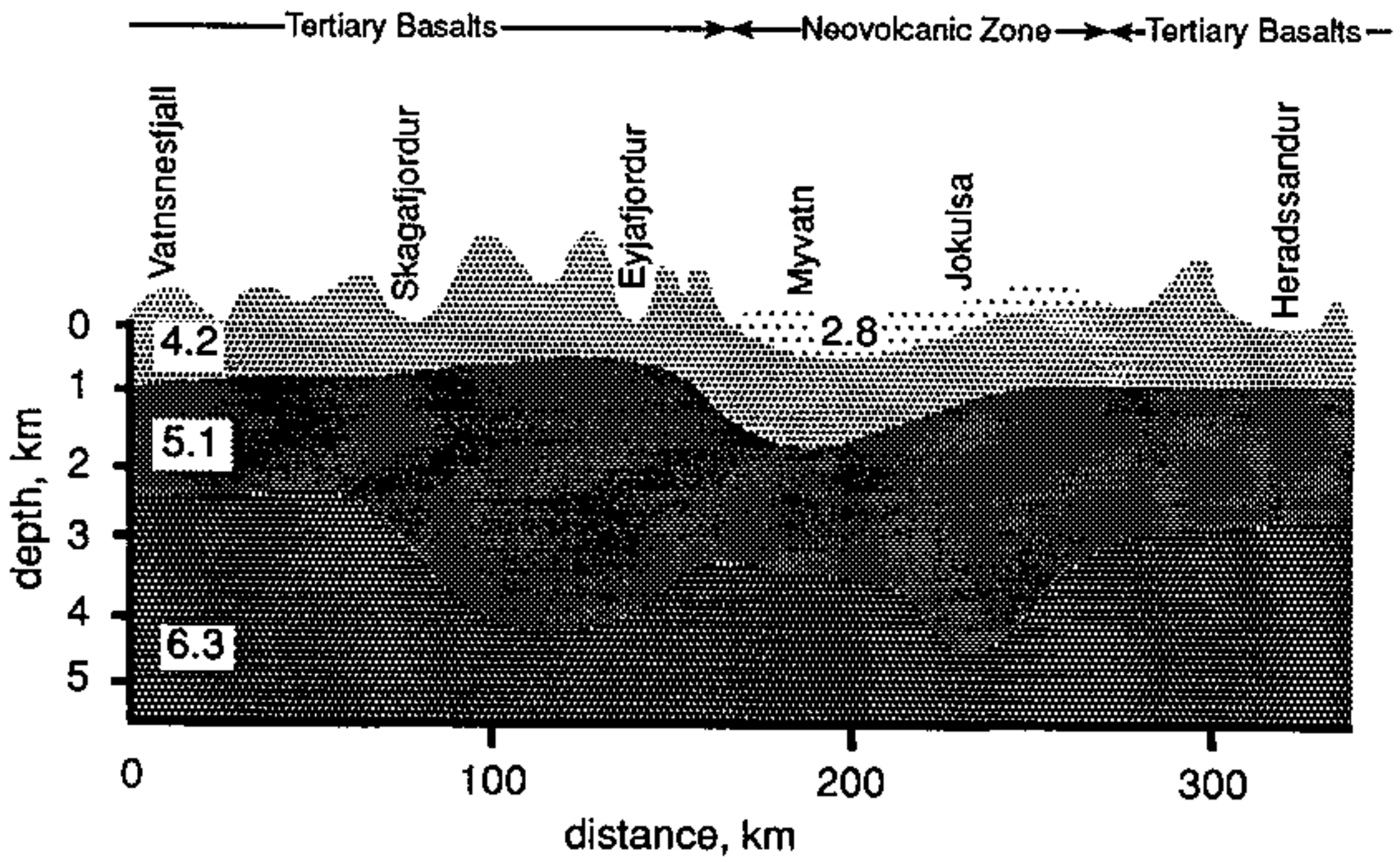
Tertiary Basalts
Neovolcanic Zone
Tertiary Basalts
Vatnsnesfjall
Skagafjordur
Eyjafjordur
Myvatn
Jokulsa
Heradssandur
4.2
2.8
5.1
6.3
depth, km
0
1
2
3
4
5
0
100
200
300
distance, km

Figure 33

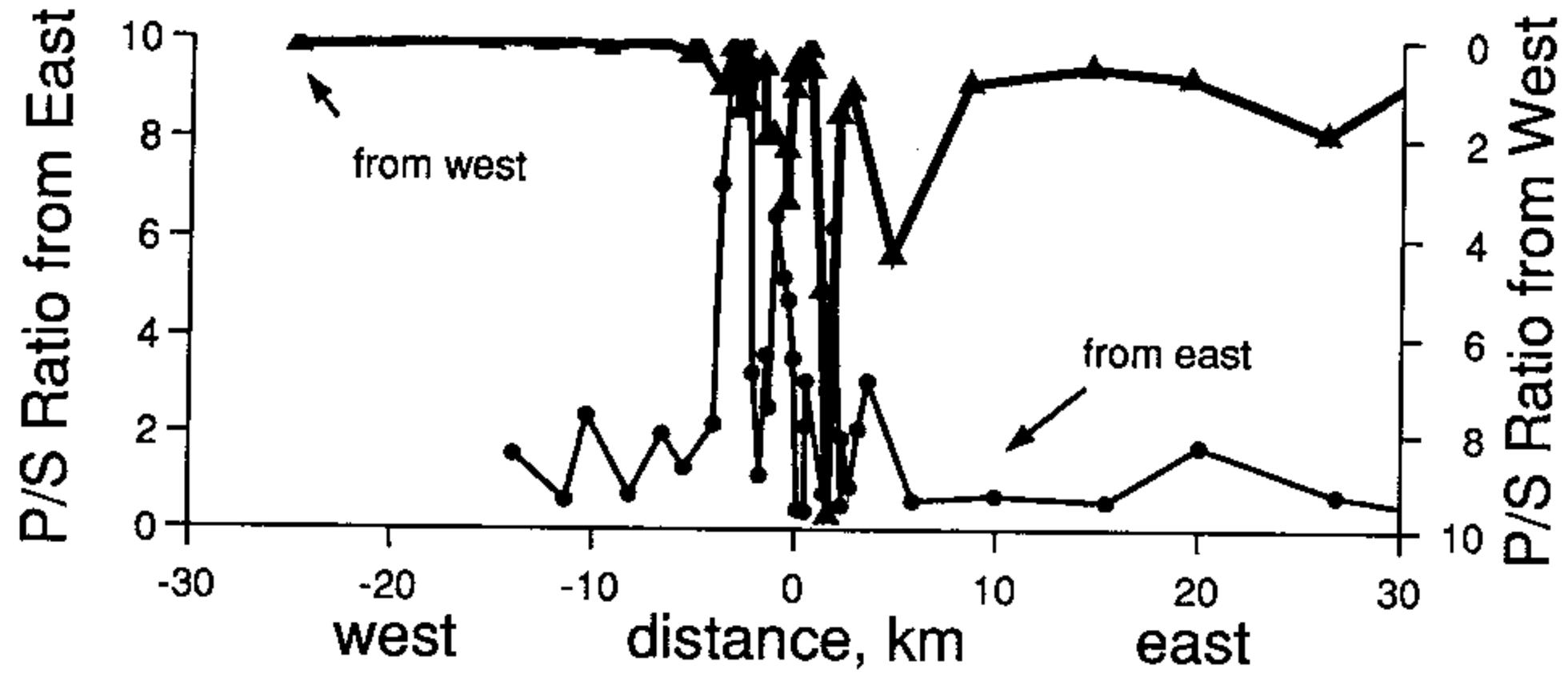
P/S Ratio from East
10
8
6
4
2
0
from west
from east
P/S Ratio from West
0
2
4
6
8
10
-30
-20
-10
0
10
20
30
west
distance, km
east

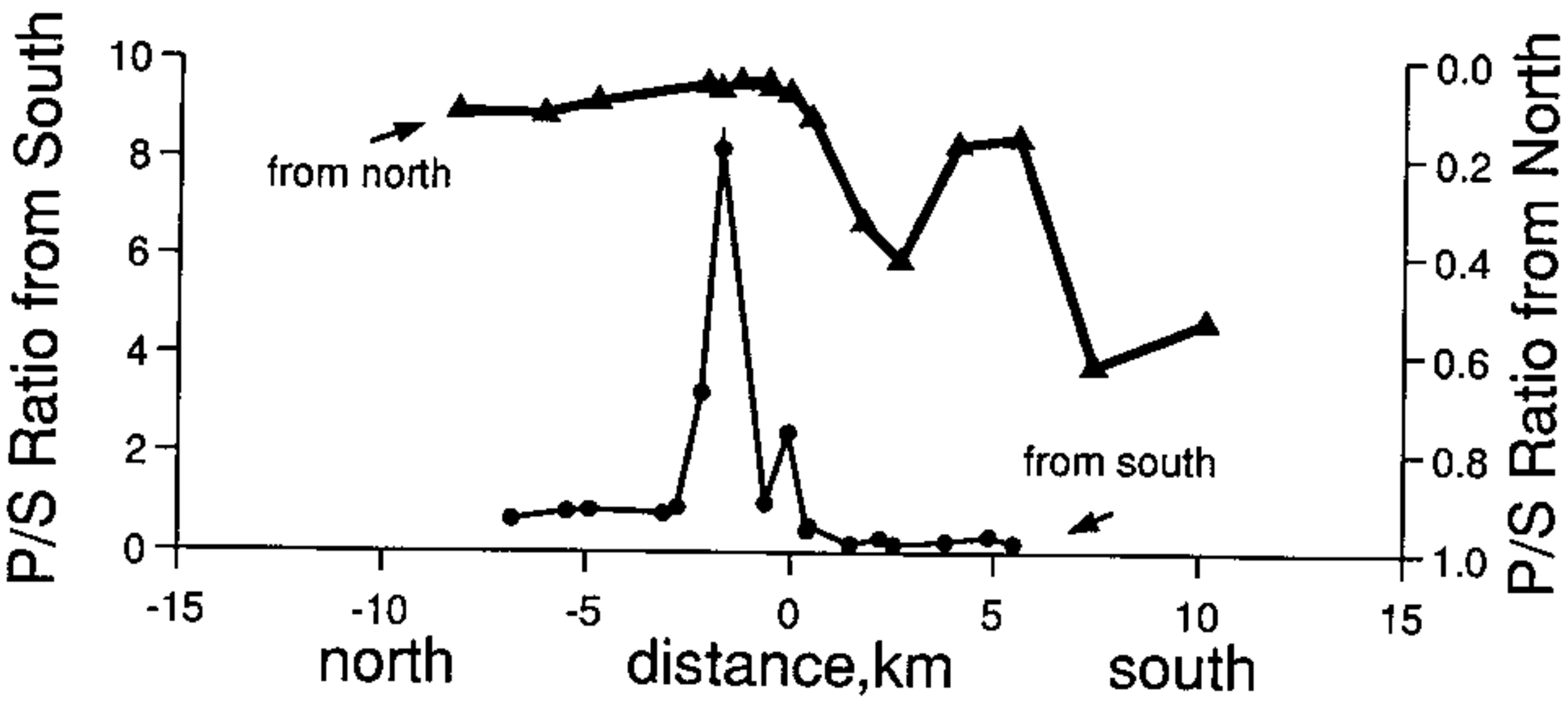
P/S Ratio from South
10
8
6
4
2
0
from north
from south
P/S Ratio from North
0.0
0.2
0.4
0.6
0.8
1.0
-15
-10
-5
0
5
10
15
north
distance,km
south

Figure 34

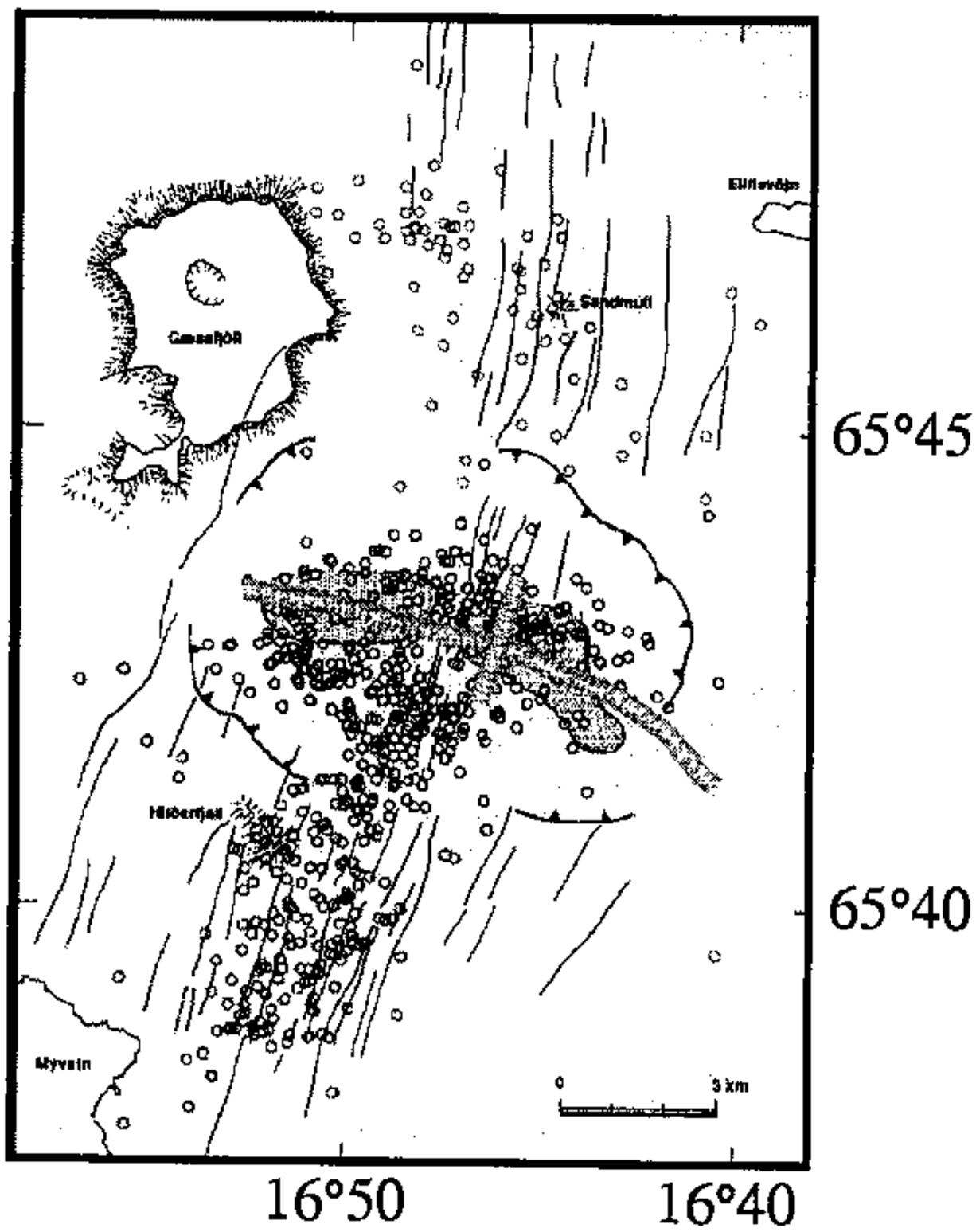
Elliðavatn
Sandmúli
Gunnhóll
Hlíðarfjall
Mývatn
0
3 km
65°45
65°40
16°50
16°40

Figure 35

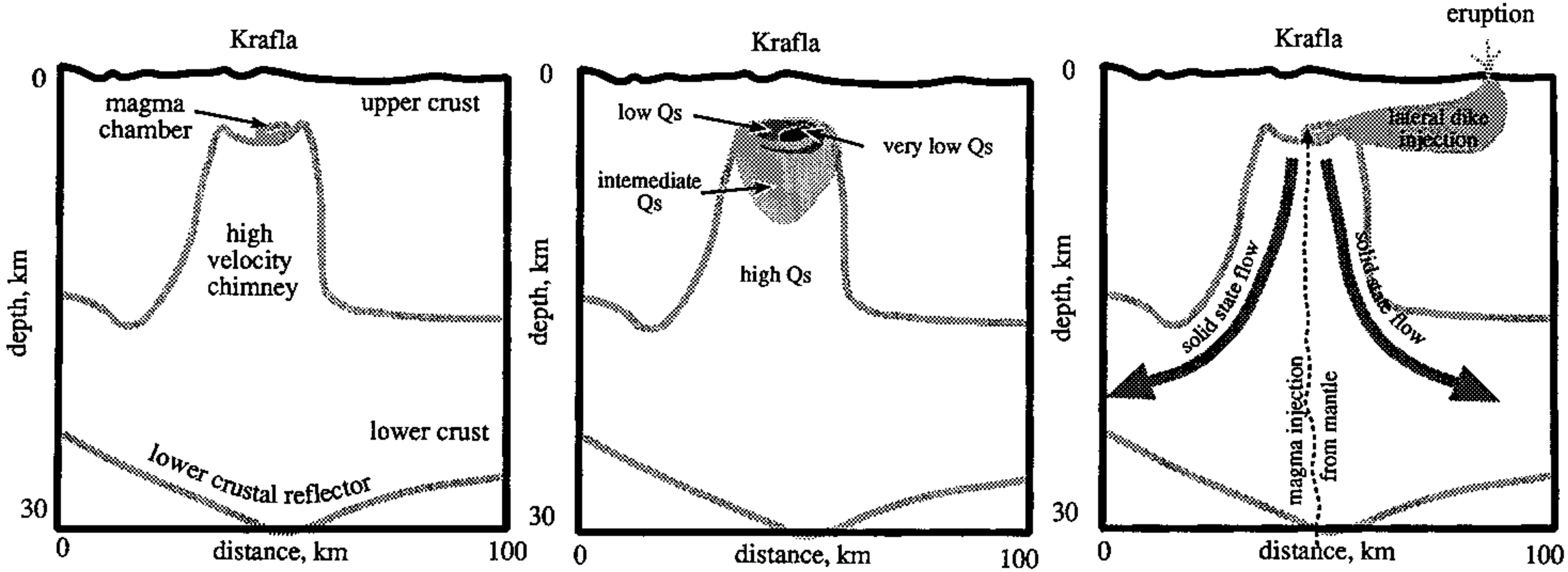
Krafla
0
magma chamber
upper crust
high velocity chimney
depth, km
lower crust
lower crustal reflector
30
0
distance, km
100
Krafla
0
low Qs
very low Qs
intemediate Qs
high Qs
depth, km
30
0
distance, km
100
eruption
Krafla
0
lateral dike injection
solid state flow
solid state flow
magma injection from mantle
depth, km
30
0
distance, km
100

Figure 36

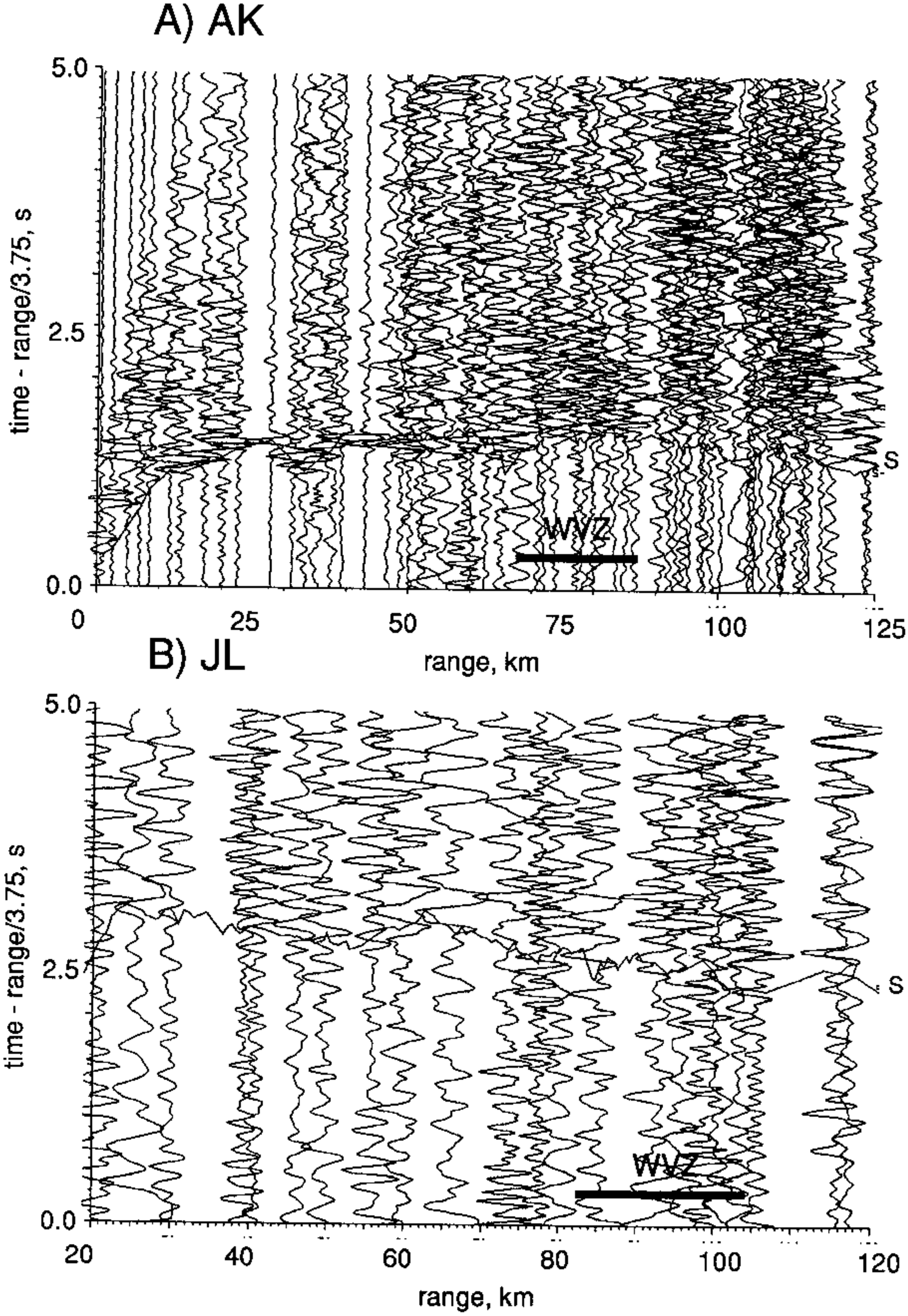
A) AK
5.0
2.5
0.0
time - range/3.75, s
0
25
50
75
100
125
range, km
S
WVZ
B) JL
5.0
2.5
0.0
time - range/3.75, s
20
40
60
80
100
120
range, km
S
WVZ

Figure 37